The Astrophysical Journal, 679:1549–1565, 2008 June 1
© 2008. The American Astronomical Society. All rights reserved. Printed in U.S.A.

THE HOBBY-EBERLY TELESCOPE CHEMICAL ABUNDANCES OF STARS IN THE HALO (CASH) PROJECT. I. THE LITHIUM-, *s*-, AND *r*-ENHANCED METAL-POOR GIANT HKII 17435−00532[1]

Ian U. Roederer,[2] Anna Frebel,[2,3] Matthew D. Shetrone,[2,3] Carlos Allende Prieto,[2] Jaehyon Rhee,[4,5] Roberto Gallino,[6,7] Sara Bisterzo,[6] Christopher Sneden,[2] Timothy C. Beers,[8] and John J. Cowan[9]

Received 2007 October 8; accepted 2008 February 21

ABSTRACT

We present the first detailed abundance analysis of the metal-poor giant HKII 17435−00532. This star was observed as part of the University of Texas long-term project Chemical Abundances of Stars in the Halo (CASH). A spectrum was obtained with the High Resolution Spectrograph (HRS) on the Hobby-Eberly Telescope with a resolving power of $R \sim 15{,}000$. Our analysis reveals that this star may be located on the red giant branch, red horizontal branch, or early asymptotic giant branch. We find that this metal-poor ($[\mathrm{Fe/H}] = -2.2$) star has an unusually high lithium abundance [$\log \varepsilon(\mathrm{Li}) = +2.1$], mild carbon ($[\mathrm{C/Fe}] = +0.7$) and sodium ($[\mathrm{Na/Fe}] = +0.6$) enhancement, as well as enhancement of both *s*-process ($[\mathrm{Ba/Fe}] = +0.8$) and *r*-process ($[\mathrm{Eu/Fe}] = +0.5$) material. The high Li abundance can be explained by self-enrichment through extra mixing that connects the convective envelope with the outer regions of the H-burning shell. If so, HKII 17435−00532 is the most metal-poor star in which this short-lived phase of Li enrichment has been observed. The Na and *n*-capture enrichment can be explained by mass transfer from a companion that passed through the thermally pulsing AGB phase of evolution with only a small initial enrichment of *r*-process material present in the birth cloud. Despite the current nondetection of radial velocity variations (over ∼180 days), it is possible that HKII 17435−00532 is in a long-period or highly inclined binary system, similar to other stars with similar *n*-capture enrichment patterns.

Subject headings: nuclear reactions, nucleosynthesis, abundances — stars: abundances — stars: individual (HKII 17435−00532) — stars: Population II

Online material: color figures, machine-readable table

1. INTRODUCTION

The story of early Galactic nucleosynthesis is written in the chemical compositions of very metal-poor halo stars. The abundances in these stars reflect only a few chemical enrichment events, and hence this fossil record can be used to trace the chemical and dynamical evolution of the early Galaxy. While the individual abundances of most metals in these stars will remain unchanged throughout the stellar lifetimes, close examination is necessary to discern exceptions to this rule.

Lithium (Li), the only metal produced during the big bang, is often observed in unevolved metal-poor stars. Information on the primordial Li abundance can be inferred from, e.g., the Spite plateau (Spite & Spite 1982) Li abundance characteristic of most warm, metal-poor turnoff and subgiant stars. A wide spectrum of Spite plateau/primordial Li abundances has been inferred from recent studies of these stars: $\log \varepsilon(\mathrm{Li}) = 2.37$ (with an observational scatter of 0.05–0.06 dex; Meléndez & Ramírez 2004), $\log \varepsilon(\mathrm{Li}) = 2.21 \pm 0.09$ (Charbonnel & Primas 2005), $\log \varepsilon(\mathrm{Li}) = 2.04$ or 2.15 (depending on the range of metallicities of the stars included in the fit, since their plateau has a metallicity dependence; Asplund et al. 2006), and $\log \varepsilon(\mathrm{Li}) = 2.10 \pm 0.09$ (Bonifacio et al. 2007).[10] Despite the wide range, the stellar result does not agree with the *WMAP* estimate of the primordial Li abundance, $\log \varepsilon(\mathrm{Li}) = 2.64 \pm 0.03$ (Spergel et al. 2007).

Metal diffusion in long-lived, low-mass stars could present a solution to the problem for globular cluster stars (Korn et al. 2006), while processing and depletion of ^{7}Li by Population III stars prior to the formation of Population II stars could explain the Li abundance found in present-day metal-poor field stars (Piau et al. 2006). Some objects, however, appear to have *overabundances* of Li, in contrast to the sparse Galactic production mechanisms of Li through cosmic-ray spallation, and in spite of the fact that Li is completely diluted and destroyed in the stellar atmosphere by the time the star reaches the giant branch.

It was first proposed by Cameron (1955) and Cameron & Fowler (1971) that ^{7}Li could be synthesized via the $^3\mathrm{He}(\alpha, \gamma)^7\mathrm{Be}$ and $^7\mathrm{Be}(e^-\nu)^7\mathrm{Li}$ reactions during the late stages of stellar evolution, when a star is ascending the asymptotic giant branch (AGB). Here the outer convection zone extends down into the H-burning shell, which is enriched in ^{3}He from proton-proton

[1] Based on observations obtained with the Hobby-Eberly Telescope, which is a joint project of the University of Texas at Austin, the Pennsylvania State University, Stanford University, Ludwig-Maximilians-Universität München, and Georg-August-Universität Göttingen.

[2] Department of Astronomy, University of Texas, Austin, TX 78712-0259; iur@astro.as.utexas.edu, anna@astro.as.utexas.edu, shetrone@astro.as.utexas.edu, callende@astro.as.utexas.edu, chris@astro.as.utexas.edu.

[3] McDonald Observatory, University of Texas, Fort Davis, TX 79734.

[4] Department of Physics, Purdue University, West Lafayette, IN 47907-2036; jrhee@physics.purdue.edu.

[5] Visiting Astronomer, Kitt Peak National Observatory, National Optical Astronomy Observatory, which is operated by the Association of Universities for Research in Astronomy (AURA), Inc., under cooperative agreement with the National Science Foundation.

[6] Dipartimento di Fisica Generale, Università di Torino, Torino, Italy; gallino@ph.unito.it, bisterzo@ph.unito.it.

[7] Centre for Stellar and Planetary Astrophysics, Monash University, Clayton, VIC 3800, Australia.

[8] Department of Physics and Astronomy, Center for the Study of Cosmic Evolution, and Joint Institute for Nuclear Astrophysics, Michigan State University, East Lansing, MI 48824; beers@pa.msu.edu.

[9] Homer L. Dodge Department of Physics and Astronomy, University of Oklahoma, Norman, OK 73019; cowan@nhn.ou.edu.

[10] We adopt the usual spectroscopic notations that $[\mathrm{A/B}] \equiv \log_{10}(N_\mathrm{A}/N_\mathrm{B})_\star - \log_{10}(N_\mathrm{A}/N_\mathrm{B})_\odot$ and that $\log \varepsilon(\mathrm{A}) \equiv \log_{10}(N_\mathrm{A}/N_\mathrm{H}) + 12.00$, for elements A and B.

chain reactions. These nucleosynthesis reactions make it indeed possible for a star to self-enrich its atmosphere with Li, but only for a very short period of time before the freshly produced Li burns again. The enrichment can be quite extreme, however, with Li abundances sometimes 1–2 dex higher than the Spite plateau value (e.g., Reddy & Lambert 2005). In the past decade or so, a number of stars at roughly solar metallicity have been discovered that exhibit high Li abundances associated with self-enrichment. These cases have been confirmed on theoretical grounds (Charbonnel & Balachandran 2000) from their distinct position on the Hertzsprung-Russell diagram.

At the heavy end of the periodic table, the neutron-capture (*n*-capture) elements are also useful diagnostics of stellar interiors and nucleosynthesis. During the last decade or so, new high-resolution echelle spectrographs on large-aperture telescopes and new laboratory measurements of atomic data have revolutionized the study of *n*-capture species in metal-poor stars (see Sneden et al. 2008 and references therein). In most cases, slow process (*s*-process) enrichment in metal-poor stars is associated with binary systems, where the primary goes through the thermally pulsing AGB (TP-AGB) phase and produces large amounts of *s*-process material. This material is transferred onto the lower mass, longer lived companion that is still observable. On the other hand, rapid process (*r*-process) enrichment observed in metal-poor stars can be associated with explosive nucleosynthesis, although the exact site of the *r*-process has not yet been conclusively identified.

Barium and europium are the heavy elements most commonly used to diagnose the *n*-capture enrichment history of a star because they are so dominantly produced by the main *s*- and *r*-processes,[11] respectively. While [Ba/Fe] or [Eu/Fe] ratios can typically reveal the overall content of *s*- and *r*-process material in a star, the [Ba/Eu] ratio gives an indication of the relative contributions of the *s*- and *r*-processes to the observed star. Because of the physical conditions necessary to produce the *n*-capture species, it is probable that *none* of the observed *n*-capture species in metal-poor stars were actually created by the star they are currently observed in. Some stars exhibit strong *s*-process enhancement, some exhibit strong *r*-process enhancement, and others exhibit significant amounts of both *s*- and *r*-process material (see Jonsell et al. 2006 and references therein).

In this paper we present HKII 17435−00532, a metal-poor star that possesses an unexpectedly high (for its evolutionary state) Li abundance, a significant amount of *s*-process material, and a smaller but nonnegligible amount of *r*-process material.

2. OBSERVATIONAL DATA AND MEASUREMENTS

2.1. *Target Selection*

The HK-II survey (Rhee 2001; J. Rhee et al. 2008, in preparation) originated as an extension of the original HK objective-prism survey of Beers et al. (1985, 1992). HK-II was designed to discover a large sample of very metal-poor *red giant* stars with $[\mathrm{Fe/H}] \leq -2.0$ by using *digitized* objective-prism spectra and Two Micron All Sky Survey (2MASS) *JHK* colors; many of these stars were likely to have been missed in the original (visual) selection of metal-poor candidates due to an unavoidable temperature bias. The HK-II survey covers more than $\sim$7000 deg^2 (1/6 of the entire sky), targeting the thick disk and halo of the Milky Way, over the magnitude range $11.0 \leq B \leq 15.5$. Ongoing medium-resolution spectroscopic follow-up has newly confirmed more than 200 red giants and subgiants with $[\mathrm{Fe/H}] \leq -2.0$ in the first sample selected from about 100 plates (J. Rhee & T. Beers 2008, in preparation).

We have recently started the Chemical Abundances of Stars in the Halo (CASH) Project with the Hobby-Eberly Telescope (HET; Ramsey et al. 1998) located at McDonald Observatory. This project aims to characterize the chemical composition of the Galactic halo by means of abundance analyses of metal-poor stars. Our goal is to build up, over the next several years, the largest high-resolution database available for these objects to investigate, inter alia, the recent claim by Carollo et al. (2007) that there is a chemical difference between the so-called "inner" and "outer" halo populations. Furthermore, frequencies of stars with particular chemical abundances will be established. The very metal-poor giants identified in HK-II are one source of targets for our HET CASH Project, and the spectrum of HKII 17435−00532[12] was taken as part of this project. The low metallicity of HKII 17435−00532 was first identified in a medium-resolution follow-up spectrum obtained in 2005 May at the 2.1 m telescope of Kitt Peak National Observatory. Additional stars and larger samples will be presented in separate papers.

2.2. *Observations and Data Reduction*

The star HKII 17435−00532 was observed on 2007 February 9 and 28 with the High Resolution Spectrograph (HRS; Tull 1998) at the HET at McDonald Observatory as part of normal queue mode scheduled observing (Shetrone et al. 2007). Our spectra have $R \sim 15,000$ and were taken through the 3″ slit with the 316g cross-disperser setting. The spectral coverage is 4120–7850 Å, with a small break from 5930 to 6030 Å resulting from the gap between the blue and red CCDs of the HRS. One 10 minute exposure was taken on each night; we scheduled the two visits at least 2 weeks apart to test for radial velocity variations.

For the reduction of all HET/HRS data obtained through the CASH Project we set up the IDL-based REDUCE data reduction software package (Piskunov & Valenti 2002). The extracted spectra were combined after correcting for any heliocentric radial velocities. Overlapping echelle orders were merged together to produce the final spectrum. The final signal-to-noise ratio (S/N) values per pixel measured from clean, line-free regions of the continuum in the REDUCE spectrum range from $\sim$50/1 at 4480 Å to $\sim$130/1 at 5730 Å to $\sim$160/1 at 6700 Å. More details on this reduction procedure for the entire HET CASH sample will be given in A. Frebel et al. (2008, in preparation).

We also reduced the data with standard IRAF[13] routines in the `echelle` and `onedspec` packages for overscan removal, bias subtraction, flat-fielding, scattered light removal, and order extraction.

[11] Two methods are commonly used to determine the relative contributions of the *s*- and *r*-processes to solar system (SS) material, the classical method (Clayton et al. 1961; Seeger et al. 1965; Käppeler et al. 1989) and the stellar model (Arlandini et al. 1999). The classical method predicts that 85% of the Ba in SS material originated in the *s*-process and that 97% of the Eu in SS material originated in the *r*-process (Simmerer et al. 2004). The stellar model predicts that 81% of the Ba in SS material originated in the *s*-process and that 96% of the Eu in SS material originated in the *r*-process.

[12] In order to distinguish two source surveys, the stars from the HK-II survey use the alphabetic prefix "HKII" while the stars from the original HK survey use the prefixes "BS" and "CS." The HK-II survey uses the exact same plates as the original HK survey, so the first five digits (following the alphabetic prefix) in the star names should be identical. However, running ID numbers (last five digits) are completely different. For example, the star HKII 17435−00532 is different from the star BS 17435−532, but HKII 17435−00532 *is* a rediscovery of the star BS 17435−012, which was noted as being a metal-poor candidate during the initial visual inspection of the HK plates.

[13] IRAF is distributed by the National Optical Astronomy Observatory, which is operated by the Association of Universities for Research in Astronomy, Inc., under cooperative agreement with the National Science Foundation.

TABLE 1
Summary of Radial Velocity Measurements

HJD	RV (km s^{-1})	Facility
2,454,140.79715	38.61 (0.64)	HET+HRS
2,454,159.73386	38.77 (0.57)	HET+HRS
2,454,297.61639	39.36 (0.59)	McD2.7m+cs21
2,454,318.60116	38.79 (1.07)	McD2.7m+cs23

Individual orders were not merged together. The final S/N values from the IRAF spectrum are very comparable to the REDUCE spectrum. Equivalent widths were also measured for 121 lines in common to the two spectra to test any systematic differences. We find a mean offset of $\Delta = -3 \pm 8$ mÅ (where Δ is defined as $EW_{REDUCE} - EW_{IRAF}$). There are no statistically significant trends with either equivalent width or wavelength between the two differently reduced sets of spectra.

To obtain additional information on the radial velocity of HKII 17435−00532, two supplemental exposures were taken on 2007 July 15 and 2007 August 5 with the Cross-Dispersed Echelle Spectrometer (Tull et al. 1995) on the Harlan J. Smith 2.7 m Telescope at $R \sim 60,000$. Reduction was performed using the standard IRAF routines. The exposure times were 1200 s, yielding S/N $\sim$ 10/1 at 4480 Å, ~20/1 at 5730 Å, and ~25/1 at 6700 Å. Since the S/N of the 2.7 m spectra is much less than the S/N of the HET/HRS spectra, these spectra were solely used for the radial velocity analysis and not for the abundance analysis.

2.3. *Radial Velocity*

The radial velocities were measured in the IRAF reduced spectrum by combining the orders covering the wavelengths 4900–5800 Å, which are mostly clear of telluric features and sky emission lines. The spectra were then cross-correlated against the Arcturus atlas (Hinkle et al. 2000) spectra using the IRAF task `fxcor` to yield a relative velocity. Heliocentric corrections were made using the IRAF task `rvcorrect`. We also cross-correlated the telluric A band against a model of this band we constructed to yield a zero-point correction to the wavelength scale; this is necessary because the ThAr fibers are separate from the science fibers in the HRS. In Table 1 we have listed the epochs of observations, as well as the resulting velocities. The weighted average velocity is 38.9 km s^{-1} with an error of the mean of 0.3 km s^{-1}. The errors in the individual velocity measurements include the systematic errors from the telluric features and the error in the relative velocity with respect to Arcturus. All of the velocity measurements are within 1 σ of the average velocity. The first and last observations of this star are spaced nearly 6 months apart, and successive observations are separated by more than 2 weeks. We find no evidence from these radial velocity measurements that HKII 17435−00532 is in a binary system. If it were in a binary, it must have a very long period and/or an amplitude smaller than $\sim$ 1.0 km s^{-1}, a result of a face-on orbit with very large sin i.

2.4. *Atmospheric Parameters*

Basic stellar data for HKII 17435−00532 are shown in Table 2. For our analysis, we use the most recent version (2002) of the LTE spectrum analysis code MOOG (Sneden 1973). We use model atmospheres computed from the Kurucz (1993) grid without convective overshooting. Interpolation software for the Kurucz grid has been kindly provided by A. McWilliam & I. Ivans (2003, private communication). We measure equivalent widths of 86 Fe I lines and six Fe II lines in HKII 17435−00532 by fitting Gaussian profiles with the SPECTRE code (Fitzpatrick & Sneden 1987). Our equivalent width measurements for all species in HKII 17435−00532 are presented in Table 3.

TABLE 2
Basic Stellar Data and Model Atmosphere Parameters

Quantity	Value	Source
R.A. (J2000.0)	$11^h49^m03.3^s$	1
Decl. (J2000.0)	$+16°58'41.7''$	1
V	13.145 ± 0.166	2
I	12.237 ± 0.067	2
J	11.534 ± 0.021	3
H	11.121 ± 0.023	3
K	11.049 ± 0.020	3
$E(B-V)$	0.042	4
$\log(L/L_\odot)$	2.01 ± 0.50	1
$T_{\rm eff}$ (K)	5200 ± 150	1
$\log g$	2.15 ± 0.4	1
v_t (km s^{-1})	2.0 ± 0.3	1
[M/H]	−1.85 ± 0.23	1
[Fe/H]	−2.23 ± 0.23	1

References.—(1) This study; (2) TASS; (3) 2MASS; (4) Schlegel et al. 1998.

The Schlegel et al. (1998) dust maps predict $E(B-V) = 0.042$ in the direction of HKII 17435−00532. This is the expected reddening value at infinite distance. At the high Galactic latitude of our halo star, $b = +73°$, its distance implies that the reddening along the line of sight to this star is essentially the reddening at infinity (see eq. [4] of Mendez & van Altena 1998). The earlier predictions of Burstein & Heiles (1982) yield $E(B-V) \lesssim 0.01$. We also attempt to use the Munari & Zwitter (1997) calibrations between the interstellar Na D1 line equivalent width and reddening. The interstellar Na D lines suffer from telluric emission and blending with the stellar lines in our HET spectra (and no simultaneous sky spectra were obtained), and these lines fall between echelle orders in our higher resolution McDonald spectra. Given these difficulties, our interstellar Na D1 equivalent width should be interpreted as an upper limit. If we naively adopt this equivalent width, the Munari & Zwitter (1997) calibrations then predict an uninteresting upper limit for the reddening of $E(B-V) \lesssim 0.12$, and larger equivalent width estimates would increase the reddening upper limit. Lacking further information, we adopt the Schlegel et al. (1998) reddening estimate.

TABLE 3
Equivalent Width Measurements

Species	Z	λ (Å)	EP (eV)	$\log gf$	EW (mÅ)
Na I	11	5682.63	2.100	−0.699	20.0
	11	5688.21	2.100	−0.456	33.0
Mg I	12	4571.10	0.000	−5.393	73.7
	12	4702.99	4.330	−0.380	113.9
	12	5183.62	2.720	−0.158	233.2
	12	5528.42	4.330	−0.500	87.0
K I	19	7698.97	0.000	−0.170	47.6
Ca I	20	4435.68	1.890	−0.520	66.7

Notes.—Table 3 is published in its entirety in the electronic edition of the *Astrophysical Journal*. A portion is shown here for guidance regarding its form and content.

We derive the effective temperature of HKII 17435−00532 from recent color-$T_{\rm eff}$ calibrations of Alonso et al. (1996, 1999). We collected V, I (TASS: The Amateur Sky Survey, ver. 2; Droege et al. 2006), J, H, and K (2MASS[14,15]; Skrutskie et al. 2006) broadband photometry measurements from the literature.[16] Using the dereddened $(V-I)$, $(J-H)$, $(J-K)$, and $(V-K)$ colors derived from TASS and 2MASS photometry, we derive a mean temperature of 5173 K with a standard deviation of 82 K.[17] To estimate the amount of systematic uncertainty, we compare with the temperature scale defined by the Ramírez & Meléndez (2005a, 2005b) $(V-J)$, $(V-H)$, and $(V-K)$ calibrations; at the metallicity of HKII 17435−00532, our $(V-I)$ falls beyond the range of applicability of their calibrations. These three color-$T_{\rm eff}$ calibrations predict a mean of 5079 K, about 100 K lower than the Alonso et al. (1999) mean. If we were to adopt zero reddening or twice the reddening predicted by the Schlegel et al. (1998) maps, our temperatures would differ by roughly 130 K. Considering all of these matters, we round the Alonso et al. (1999) predicted temperature to 5200 K and adopt a conservative total uncertainty of 150 K.

Our method for deriving the surface gravity requires that, for our adopted effective temperature, the abundances derived from neutral and ionized lines of Fe agree. We neglect the effects of non-LTE (NLTE) line formation, which may affect the Fe I abundance measurements at the ∼0.1 dex level (e.g., Asplund 2005). The microturbulence is measured by requiring that the abundances derived from strong and weak lines of Fe I agree. These parameters are varied iteratively until we arrive at our final values. [Fe/H] is defined by the Fe abundance for the final set of $T_{\rm eff}$, $\log g$, and v_t. We increase the overall metallicity Z of the atmosphere by +0.4 dex to account for the extra electrons from the α-elements that contribute to the H^- continuous opacity; this artificial increase alters our derived abundances of the electron-donating elements by $\lesssim$0.01 dex and is completely negligible when elemental abundance ratios are considered (see, e.g., § 4.3 of Roederer et al. 2008). We adopt the following atmospheric parameters for HKII 17435−00532: ($T_{\rm eff}$, $\log g$, v_t, [Fe/H]) = (5200 K, 2.15, 2.0 km s^{-1}, −2.23). These values are also displayed in Table 2.

An alternate method for deriving $T_{\rm eff}$, $\log g$, and [Fe/H] uses the HET calibration sample for the Sloan Digital Sky Survey to fit a region around the Mg I b triplet (see discussion in Allende Prieto et al. 2008). For the sum of the two individual spectra of HKII 17435−00532, this method finds ($T_{\rm eff}$, $\log g$, [Fe/H]) = (4978 ± 72 K, 2.06 ± 0.13, −2.26 ± 0.06). While the gravity and metallicity are in good agreement with our spectroscopic values, the temperature is about 200 K cooler. The gravity obtained from the Fe ionization balance is also not well constrained because we are only able to measure equivalent widths of six Fe II lines, and we adopt an uncertainty of ±0.4 in $\log g$. We also adopt ±0.3 km s^{-1} as the uncertainty in v_t. The uncertainty in the metallicity, ±0.23 dex, is found by combining the uncertainties in the other atmospheric parameters and the line-to-line Fe I abundance scatter in quadrature.

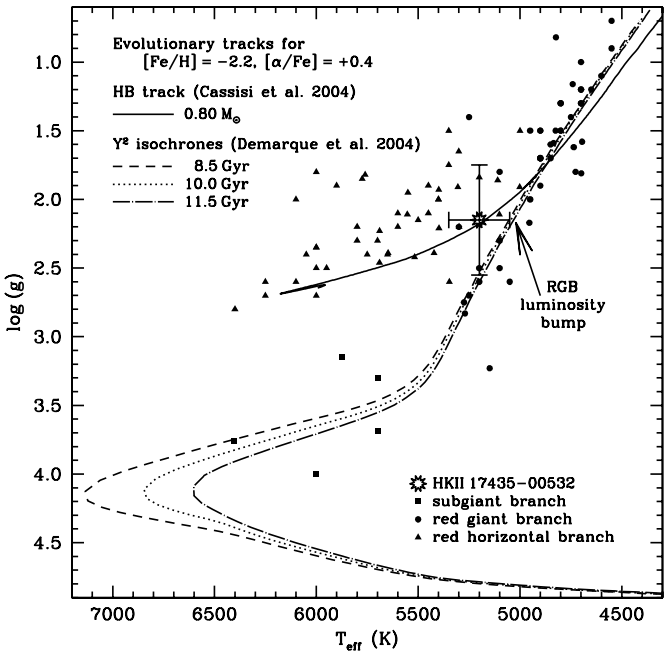

FIG. 1.—Spectroscopic gravities as a function of effective temperature for HKII 17435−00532 and a sample of other evolved metal-poor stars from previous studies. HKII 17435−00532 is indicated by the sunburst. The evolved sample is compiled from the data in Behr (2003; only stars with [Fe/H] < −1.0), Cayrel et al. (2004), and Preston et al. (2006). Filled squares indicate stars classified as "turnoff" or "subgiant" stars, filled circles indicate stars classified as being on the RGB, and filled triangles indicate stars classified as being on the RHB. We also display several evolutionary tracks for reference, which have all been computed for [Fe/H] = −2.2 and [α/Fe] = +0.4. Three sets of Y^2 isochrones (Demarque et al. 2004) are displayed, corresponding to ages of 8.5 Gyr (*dashed line*), 10.0 Gyr (*dotted line*), and 11.5 Gyr (*dot-dashed line*). The assumed age has little effect on the location of the RGB. A synthetic HB (Cassisi et al. 2004) for $M = 0.80\ M_\odot$ is shown by the solid line. Small changes in the assumed mass have little effect on the location of the HB. The arrow indicates the location of the RGB luminosity bump. [*See the electronic edition of the Journal for a color version of this figure.*]

3. EVOLUTIONARY STATUS OF HKII 17435−00532

The location of HKII 17435−00532 on the $T_{\rm eff}$–$\log g$ diagram is shown in Figure 1. We plot the spectroscopically determined gravity as a function of effective temperature for HKII 17435−00532 and many other evolved stars collected from previous studies. HKII 17435−00532 is located in the region of the diagram that is populated by metal-poor stars that have been classified as being on the red giant branch (RGB) and stars that have been classified as being on the red horizontal branch (RHB). For reference, we also display evolutionary tracks in Figure 1. The Y^2 isochrones (Demarque et al. 2004) for three different ages (8.5, 10.0, and 11.5 Gyr) with metallicity [Fe/H] = −2.2 and [α/Fe] = +0.4, similar to that of our star, are shown. As can be seen, these isochrones approximately match the positions of the stars on the subgiant and red giant branches. For an old, metal-poor population of giants, it is clear that the assumed age has no effect on their location in the $T_{\rm eff}$–$\log g$ diagram.

[14] This research has made use of the NASA/IPAC Infrared Science Archive, which is operated by the Jet Propulsion Laboratory, California Institute of Technology, under contract with the National Aeronautics and Space Administration.

[15] This publication makes use of data products from the Two Micron All Sky Survey, which is a joint project of the University of Massachusetts and the Infrared Processing and Analysis Center/California Institute of Technology, funded by the National Aeronautics and Space Administration and the National Science Foundation.

[16] New *BVRI* broadband photometry of HKII 17435−00532 was obtained by T. Chonis and M. Gaskell after our analysis was completed. The $(V-I)$ color computed from this work, 0.902, is in superb agreement with the $(V-I)$ color computed from the TASS photometry, 0.908. This agreement reinforces our confidence in the reliability of the colors employed for our photometric temperature determination, especially in light of the rather large uncertainty in the V magnitude from TASS, $V = 13.145 \pm 0.166$.

[17] If we include the $(B-V)$, $(V-R)$, and $(R-I)$ colors from the new *BVRI* photometry described in footnote 16 in place of TASS photometry, the mean of the seven calibrations rises to 5200 K. Despite the dangers of mixing sources of *BVRI* photometry, if we adopt B and R from the new photometry and V and I from TASS, the mean only changes slightly to 5228 K.

We also show a synthetic horizontal branch (HB) track (Cassisi et al. 2004) for $M = 0.80\ M_{\odot}$. At low metallicity, these tracks are only available for $Y = 0.23$, $[\alpha/\mathrm{Fe}] = 0.0$, and limited values of the metallicity Z. To scale Z of these tracks for an α-enhancement of +0.4, we use the formula given in Kim et al. (2002; see also, e.g., Salaris et al. 1993). A metallicity $[\mathrm{Fe/H}] \approx -2.2$ with $[\alpha/\mathrm{Fe}] = +0.4$ corresponds to $Z \approx 2.6 \times 10^{-4}$, which we obtain from the Cassisi et al. (2004) tracks by interpolation between the $Z = 1 \times 10^{-4}$ and $Z = 3 \times 10^{-4}$ tracks. We follow the prescription given in Preston et al. (2006) to convert the $\log (L/L_{\odot})$ given by Cassisi et al. (2004) to $\log (g/g_{\odot})$. On the scale of this figure, the location of the HB is very insensitive to small changes in the assumed mass for stars on the HB. Preston et al. (2006) performed a comparison of several different sets of HB tracks to the Cassisi et al. (2004) set. They found differences in $\log L$ (which is equivalent to $-\log g$) to be $\lesssim 0.15$ dex, which is well within the uncertainty in our $\log L$ determination for HKII 17435−00532.

HKII 17435−00532 coincidentally appears to lie on the $M = 0.80\ M_{\odot}$ HB track; however, due to the large uncertainties in our determination of the temperature and surface gravity of this star, we cannot draw any firm conclusions from this. This star could possibly be ascending the RGB for the first time or ascending the early AGB from the HB. A higher gravity or cooler temperature would place the star on the RGB. A lower gravity or warmer temperature would place the star above the $M = 0.80\ M_{\odot}$ HB track in the region of the diagram populated by (presumably) lower mass RHB stars (cf. Fig. 15 of Preston et al. 2006). This is reasonable because other metal-poor stars are found in this region. HKII 17435−00532 cannot be in the TP-AGB phase, which would require $\log g \lesssim 0.9$ and $T_{\mathrm{eff}} \lesssim 4800$ K (see, e.g., Fig. 3 of Masseron et al. 2006). To achieve Fe ionization balance at $\log g = 0.9$ would require an NLTE correction of roughly −0.5 dex to the Fe I abundance, which is much greater than has been suggested by Asplund (2005).

From fundamental relations, we calculate $\log (L/L_{\odot}) = 2.01 \pm 0.50$ for HKII 17435−00532, assuming $M = 0.8 \pm 0.1\ M_{\odot}$ for this star and $T_{\mathrm{eff}} = 5780$ K and $\log g = 4.44$ for the Sun. The uncertainty in $\log L$ is dominated by our uncertainty in the gravity.

4. VALIDATION OF OUR ABUNDANCE ANALYSIS TECHNIQUES

We chose suitable elemental lines for our abundance analysis in the range of ∼4120–7850 Å from the extensive line lists of six recent studies of abundances in very metal-poor stars (Fulbright 2000; Cayrel et al. 2004; Honda et al. 2004b; Barklem et al. 2005; Ivans et al. 2006; Frebel et al. 2007). We adopt the $\log gf$ values employed by these studies for all species except Cr I, whose $\log gf$ values were recently redetermined by Sobeck et al. (2007). To confirm the integrity of our line list and validate our abundance analysis method for measuring chemical compositions, we carried out a basic abundance analysis of the well-studied cool giant HD 122563 and the warm main-sequence turnoff star HD 84937. The spectra have $R \sim 80,000$, very high S/N, and were taken from the VLT UVES archive.

We measure equivalent widths for 227 Fe I and 35 Fe II lines in HD 122563 and 197 Fe I and 26 Fe II lines in HD 84937. We derive $(T_{\mathrm{eff}}, \log g, v_t, [\mathrm{Fe/H}]) = (4570 \pm 100\ \mathrm{K}, 0.85 \pm 0.3, 2.0 \pm 0.3\ \mathrm{km\ s^{-1}}, -2.81 \pm 0.15)$ for HD 122563 and $(6300 \pm 100\ \mathrm{K}, 4.0 \pm 0.3, 1.2 \pm 0.3\ \mathrm{km\ s^{-1}}, -2.28 \pm 0.12)$ for HD 84937 using the methods described in § 2.4. In Table 4 we compare our derived parameters with a number of other recent high-resolution studies. For both HD 122563 and HD 84937, each of our derived parameters agrees with the mean from other studies within their mutual 1 σ uncertainties.

TABLE 4
Comparison of Model Atmosphere Parameters

Reference	T_{eff} (K)	$\log g$	v_{micro} (km s^{-1})	[Fe/H]
HD 122563				
This study	4570	0.85	2.0	−2.81
Aoki et al. (2005)	4600	1.1	2.2	−2.62
Barbuy et al. (2003) model 1	4600	1.5	2.0	−2.71
Barbuy et al. (2003) model 2	4600	1.1	2.0	−2.80
Fulbright (2000)	4425	0.6	2.75	−2.60
Fulbright & Johnson (2003)	4650	1.24	1.85	−2.63
Honda et al. (2004a)	4570	1.1	2.2	−2.77
Johnson (2002)	4450	0.50	2.3	−2.65
Mishenina & Kovtyukh (2001)	4570	1.1	1.2	−2.42
Roederer et al. (2008)	4570	0.55	2.4	−2.83
Takada-Hidai et al. (2005)	4650	1.36	1.9	−2.65
Thevenin (1998)	4582	0.8	2.4	−2.60
Westin et al. (2000)	4500	1.3	2.5	−2.70
Mean	4564	1.03	2.14	−2.66
Standard deviation	69	0.33	0.40	0.11
HD 84937				
This study	6300	4.0	1.2	−2.28
Bihain et al. (2004)	6277	4.03	1.0	−2.06
Fulbright (2000)	6375	4.1	0.8	−2.0
Gratton et al. (2003)	6290	4.02	1.25	−2.18
Jonsell et al. (2005)	6310	4.04	1.5	−1.96
Mishenina & Kovtyukh (2001)	6250	3.8	1.5	−2.00
Nissen et al. (2007)	6357	4.07	1.5	−2.11
Smith et al. (1993)	6090	4.0	1.5	−2.4
Thevenin (1998)	6222	4.0	1.3	−2.10
Zhang & Zhao (2005)	6261	4.07	1.8	−1.93
Mean	6270	4.01	1.35	−2.08
Standard deviation	75	0.09	0.30	0.14

Note.—The mean and standard deviation calculations do not include the values derived in this study.

We also measure 204 equivalent widths for 17 other species ($11 \leq Z \leq 30$) in HD 122563 and 161 equivalent widths for 16 other species in HD 84937. In Figure 2 we compare our derived abundances in these two stars with the abundances derived by two previous studies.

In HD 122563, the derived abundances agree with the Honda et al. (2004a, 2004b) abundances within the uncertainties for all species except Cr, Ni, and Cu, which differ by −0.29, +0.27, and −0.44 dex, respectively, where the differences are in the sense of (our study) − (other study). We measured equivalent widths for 16 Cr I lines and five Cr II lines, whereas Honda et al. (2004a, 2004b) only used three and two lines of these species, respectively. For Cr, only 0.02 dex of the difference can be accounted for by our use of updated Cr I $\log gf$ values from Sobeck et al. (2007). Another 0.14 dex results from the different atmospheric parameters derived in these two studies. This is sufficient to bring the two Cr abundance measurements into agreement within the uncertainties. Honda et al. (2004a, 2004b) derive the Ni abundance from two strong lines, whereas we measure 21 Ni lines. The equivalent widths of the two lines common to both studies are in good agreement; therefore, we attribute the discrepancy in the derived Ni abundances to the number of lines measured. The Cu abundance in both the Honda et al. (2004a, 2004b) studies and our study was measured from the Cu I line at 5105 Å; the difference in the derived abundances can be traced to the different

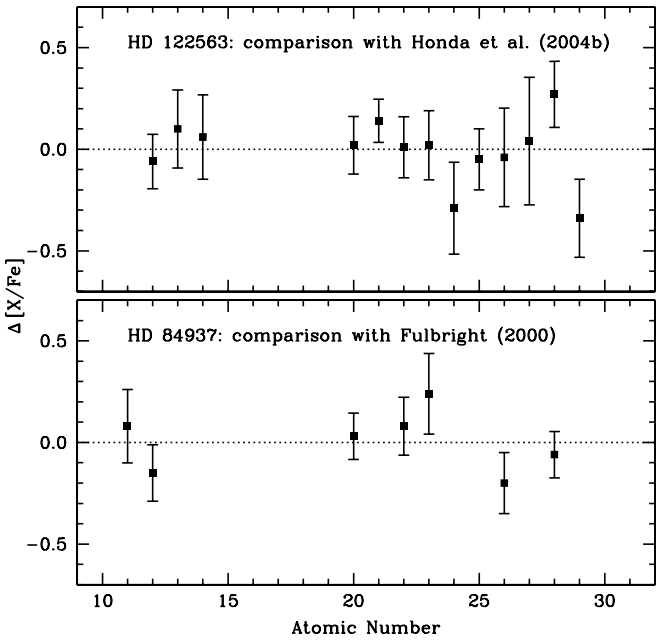

FIG. 2.— Comparison of the abundances derived in our study and two previous studies of HD 122563 and HD 84937, Honda et al. (2004a, 2004b) and Fulbright (2000). Δ[X/Fe] is in the sense of (our study) − (other study). For Fe, we show Δ[Fe/H] rather than Δ[X/Fe].

equivalent width measurements of this very weak line, 3.3 and 1.7 mÅ, respectively.

In HD 84937, the derived abundances agree with the Fulbright (2000) abundances within the uncertainties for all species except Mg, V, and Fe, which differ by −0.15, +0.24, and −0.20 dex, respectively, again in the sense of (our study) − (other study). We selected the Fulbright (2000) study for comparison because, in our efforts to compare with a set of homogeneous measurements, it offered the most elements in common with our measurements. The Mg and V abundance discrepancies can be explained by the different atmospheric parameters, which account for 0.04 and 0.06 dex of the difference, respectively, reducing the discrepancies to less than the uncertainties. When compared with many other studies (in Table 4), our [Fe/H] is in agreement with these studies within their mutual 1 σ uncertainties, so we do not consider it to be discrepant.

We also smooth the UVES spectra of HD 122563 and HD 84937 to $R \sim 15{,}000$ to simulate the spectral resolving power employed in our study. We do not degrade the S/N of these spectra to match the S/N of our HET spectra; the purpose of smoothing the spectra is to allow us to identify lines that are blended at the lower spectral resolution and remove them from our final line list. We accomplish this by noting the spuriously high abundances produced by the blended lines in a line-by-line comparison with the abundances derived from the higher resolution spectra. We then measure equivalent widths from unblended lines in each star and rederive elemental abundances using the same atmospheric parameters. The abundance ratios for both stars are identical to the abundance ratios determined from the $R \sim 80,000$ spectra within the measurement uncertainties. From this and other comparisons given above, we conclude that our line list and abundance analysis technique are reliable.

5. ABUNDANCE ANALYSIS

5.1. *Comments on Individual Species*

In Table 5 we list our derived LTE abundances, along with NLTE corrections when available, for 23 elements in HKII 17435−00532. We reference the elemental abundance ratios to the solar photospheric abundances given by Grevesse & Sauval

TABLE 5
ABUNDANCE SUMMARY FOR HKII 17435−00532

Species	LTE $\log \varepsilon$	NLTE $\log \varepsilon$	LTE [X/Fe][a]	σ	Number of Lines	$\log \varepsilon_\odot$[a]	Notes
Fe I	5.27	...	−2.23[b]	0.23	86	7.50	EW
Fe II	5.27	...	−2.23[b]	0.17	6	7.50	EW
Li I	2.06	2.16	...	0.16	1	1.10	Synth
C	6.97	...	+0.68	0.3	...	8.52	Synth
O I	7.56	∼7.2	+1.06	0.27	3	8.73	EW
Na I	4.79	∼4.7	+0.69	0.16	2	6.33	EW
Mg I	5.77	∼5.9	+0.42	0.25	4	7.58	EW
K I	3.33	∼2.9	+0.44	0.17	1	5.12	EW
Ca I	4.56	...	+0.43	0.19	13	6.36	EW
Sc II	1.14	...	+0.20	0.21	3	3.17	EW
Ti I	3.01	...	+0.22	0.22	9	5.02	EW
Ti II	3.12	...	+0.33	0.20	9	5.02	EW
Cr I	3.29	...	−0.15	0.16	4	5.67	EW
Mn I	2.85	...	−0.31	0.24	1	5.39	EW
Ni I	4.13	...	+0.11	0.18	3	6.25	EW
Sr II	1.05	...	+0.36	0.26	1	2.92	Synth
Y II	0.18	...	+0.17	0.19	4	2.24	Synth
Zr II	1.14	...	+0.77	0.27	2	2.60	Synth
Ba II	0.76	...	+0.86	0.29	4	2.13	Synth
La II	−0.28	...	+0.78	0.21	6	1.17	Synth
Ce II	0.52	...	+1.17	0.20	4	1.58	Synth
Pr II	−0.42	...	+1.10	0.20	3	0.71	Synth
Nd II	0.31	...	+1.04	0.19	12	1.50	Synth
Sm II	−0.49	...	+0.73	0.22	3	1.01	Synth
Eu II	−1.24	...	+0.48	0.20	2	0.51	Synth

[a] Solar photospheric values from Grevesse & Sauval (2002).
[b] [Fe/H] is shown here.

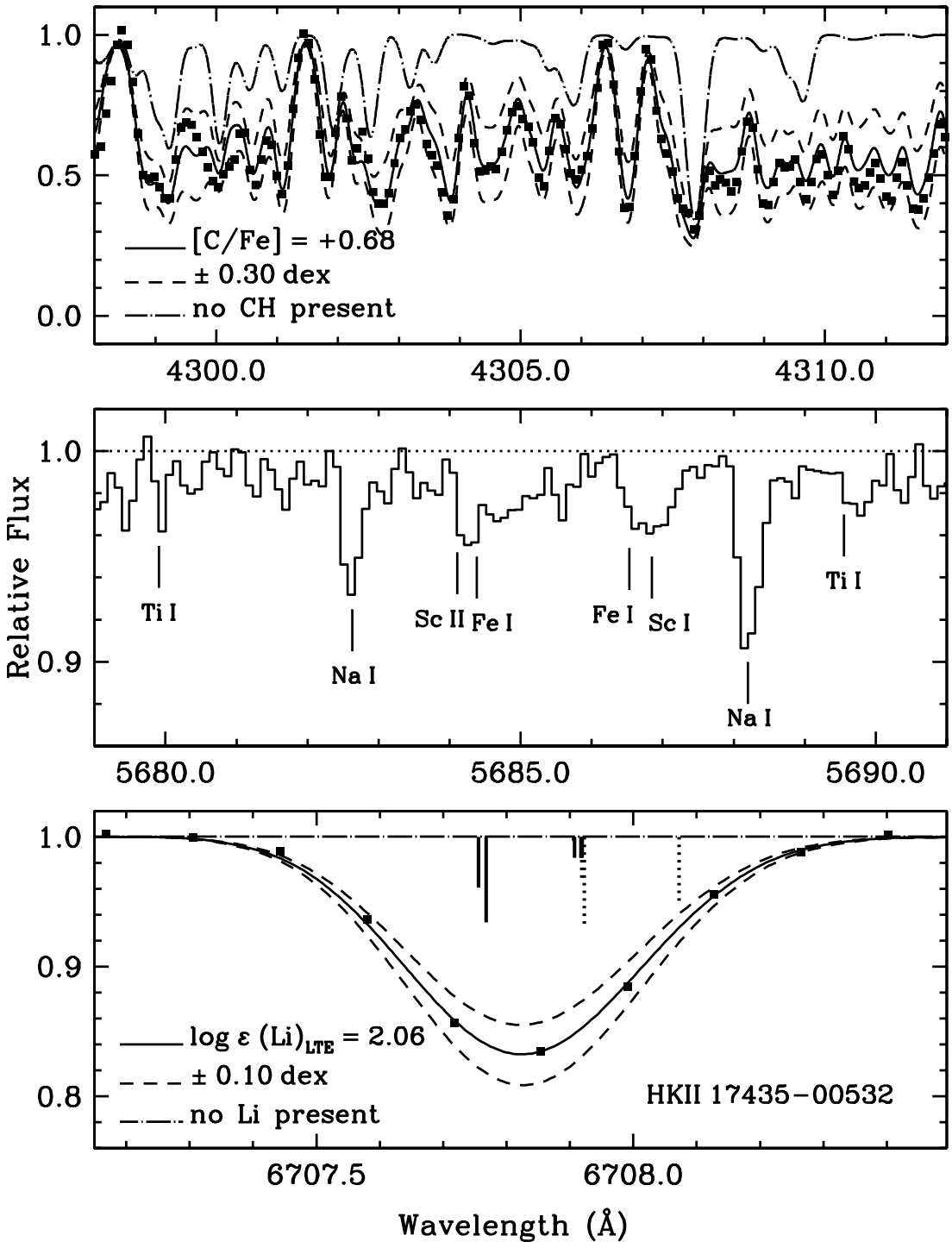

FIG. 3.—Portions of our spectrum of HKII 17435−00532. The top panel displays part of our synthesis of the CH G band near 4300 Å, the middle panel shows the spectral window around the Na I $\lambda\lambda$5682 and 5688 lines, and the bottom panel shows our synthesis of the Li I λ6707 resonance line. In the top and bottom panels, the solid line represents our best-fit synthesis, while the dashed lines represent variations in the best-fit abundance. The dot-dashed line represents a synthesis with no CH or Li present. The observed spectrum is indicated by filled squares. In the middle panel, the observed spectrum is indicated by the histogram and the dotted line indicates the location of the continuum. In the bottom panel, the relative strengths and positions of the hyperfine components of ^{7}Li are represented by solid line segments, while the ^{6}Li components are represented by dotted line segments. We can assume that only ^{7}Li is present without altering any of our conclusions. [*See the electronic edition of the Journal for a color version of this figure.*]

(2002). These abundances have been derived primarily from analyses using one-dimensional (1D) hydrostatic model atmospheres under the assumption of LTE, as we have done in our current study of HKII 17435−00532.

We synthesize the Li I λ6707 doublet using the line list of Hobbs et al. (1999), who compiled the hyperfine structure component wavenumbers of this resonance line from measurements by Sansonetti et al. (1995) and the oscillator strength measurements of Yan et al. (1998). For the purposes of this paper, we can assume that all of the Li present is ^{7}Li without altering any of our conclusions. Our synthesis of this line is shown in Figure 3. We derive $\log \varepsilon(\mathrm{Li})_{\mathrm{LTE}} = 2.06$. Using the Carlsson

et al. (1994) NLTE corrections for the λ6707 line, we find $\log \varepsilon(\mathrm{Li})_{\mathrm{NLTE}} = 2.16 \pm 0.16$.

We synthesize portions of the CH G band between 4290 and 4330 Å to determine the C abundance. A portion of this region is shown in Figure 3. We adopt the CH line list of B. Plez (2006, private communication). Because our C abundance is derived from molecular features that are very temperature sensitive in a 1D model atmosphere, it is likely that the true C abundance is somewhat lower, as has been found by Asplund et al. (2005) when analyzing atomic and molecular C features in the solar spectrum using three-dimensional (3D) hydrodynamical model atmospheres. We cannot estimate the $^{12}C/^{13}C$ ratio from the CH G band at our spectral resolution and S/N levels.

The [O I] lines at 6300 and 6363 Å, usually taken as the best O abundance indicator in metal-poor stars, are contaminated by telluric features. We measure equivalent widths for the O I triplet at 7771, 7774, and 7775 Å, adopt the log gf values from Wiese et al. (1996), and find $\log \varepsilon(\mathrm{O})_{\mathrm{LTE}} = 7.56 \pm 0.27$. As summarized in Kiselman (2001), the line source function for this triplet will show strong departures from LTE, always in the direction of underestimating the line strength and hence overestimating the abundance in LTE relative to NLTE. Kiselman (2001) adopts an NLTE correction of roughly -0.1 dex for solar-type stars with a similar O abundance, Nissen et al. (2002) found corrections of roughly -0.1 to -0.2 dex for metal-poor main-sequence and subgiant stars, and García Pérez et al. (2006) found corrections of roughly -0.1 dex for metal-poor subgiant and giant stars. García Pérez et al. (2006) also found that the O abundances derived from the triplet were roughly +0.1–0.3 dex higher than when derived from the [O I] lines for stars in their sample with a temperature similar to HKII 17435−00532; this difference is also presumably due to NLTE effects. Cavallo et al. (1997) found a similar effect in their sample of metal-poor subdwarfs and giants, and they reported a difference of +0.53 dex between the triplet and the [O I] lines. Adding the two corrections adopted from García Pérez et al. (2006), we arrive at a total NLTE correction for HKII 17435−00532 of roughly -0.3 to -0.4 dex. We therefore derive $\log \varepsilon(\mathrm{O})_{\mathrm{NLTE}} \sim 7.2$ dex for HKII 17435−00532.

Both lines in the Na I doublet at 5889 and 5895 Å are blended with interstellar absorption lines and telluric emission lines. The relative radial velocity of HKII 17435−00532 at the time of our observations does not allow us to separate these components from the stellar absorption lines. Instead, we measure equivalent widths from the Na I lines at 5682 and 5688 Å. The spectral region around these lines is shown in Figure 3. Gratton et al. (1999) offer NLTE corrections for these lines in metal-poor giants, but Asplund (2005) notes that their corrections for giants are at odds with other calculations for these lines. Gehren et al. (2004) studied the NLTE abundances of only dwarfs and early subgiants, so we cannot infer corrections from their work. Takeda et al. (2003) suggest that NLTE effects for these lines will be relatively small ($\lesssim -0.1$ dex).

We derive Mg I abundances from equivalent width measurements of four lines. NLTE corrections for two of these lines, $\lambda\lambda$4571 and 5183, have been presented by Gratton et al. (1999), who estimate corrections of roughly +0.1–0.15 dex in metal-poor giants. Gehren et al. (2004) found corrections for dwarfs and subgiants with similar metallicity to HKII 17435−00532 that are roughly +0.1 dex.

We measure an equivalent width from the K I resonance line at 7698 Å. The electron structure of K I is similar to Na I; therefore, both elements will be sensitive to similar NLTE effects in stellar atmospheres (Bruls et al. 1992). We use the interpolation software kindly provided by Y. Takeda (2007, private communication) to estimate the NLTE correction from the analysis performed by Takeda et al. (2002). The correction is rather large, roughly -0.4 dex.

We do not adopt any NLTE corrections for the remaining six light species that were detected: Ca, Sc, Ti, Cr, Mn, and Ni.

We measure abundances for 10 n-capture elements (Sr, Y, Zr, Ba, La, Ce, Pr, Nd, Sm, and Eu) in HKII 17435−00532 by generating synthetic spectra for each line. Relative wavelengths for the hyperfine structure and isotopic components were drawn from McWilliam (1998) for the Ba II λ4554 resonance line. All La II lines were synthesized with the hyperfine structure presented in Lawler et al. (2001a) and Ivans et al. (2006). Pr II lines were synthesized from the hyperfine A constants presented in Ivarsson et al. (2001). Both Eu II lines were synthesized with the hyperfine structure presented in Lawler et al. (2001b) and Ivans et al. (2006). Each of these species has notable hyperfine splitting, and thus it is necessary to synthesize the hyperfine structure and isotope shifts in order to derive accurate abundances. Our spectrum of HKII 17435−00532 does not extend far enough into the blue to observe the stronger transitions from many of the heavier n-capture species, such as the Pb I λ4057 line. We note that no Tc is detected at the $\lambda\lambda$4238, 4262, and 4297 lines in HKII 17435−00532, and we only obtain an upper limit of $\log \varepsilon(\mathrm{Tc}) \lesssim +0.5$.

5.2. *Uncertainties*

Total uncertainties in the derived elemental abundances were estimated by adding uncertainties in the log gf values, uncertainties in the EW resulting from continuum placement, the statistical scatter associated with measuring multiple lines of each species, and changes in the derived abundance in response to our uncertainties in the atmospheric parameters in quadrature. The statistical scatter is $\sim$0.1–0.2 dex for most species with more than $\sim$5 lines analyzed; for species with fewer than $\sim$5 lines, the uncertainty in the continuum placement for individual lines was found to contribute $\sim$0.1–0.2 dex to the overall abundance error budget. For neutral species, the effective temperature uncertainties translate into abundance uncertainties $\sim$0.15 dex, and for singly ionized species the surface gravity uncertainties translate into abundance uncertainties $\sim$0.10 dex. For a few species with several strong lines (Mg, Ca, Fe, Ti, and Ni), the microturbulent velocity uncertainties translate into abundance uncertainties $\sim$0.05 dex. Uncertainties in the log gf values and overall metallicity of the model atmosphere result in abundance uncertainties $\lesssim$0.05 dex. One extreme case is C, whose abundance was derived from molecular CH bands; a change in T_{eff} by $\pm$150 K changes the C abundance by approximately $\pm$0.30 dex, which dominates over changes in the other atmospheric parameters.

6. RESULTS

6.1. *Lithium*

Contrary to expectations from the evolved nature of HKII 17435−00532, we have detected the Li λ6707 line, deriving an abundance of $\log \varepsilon(\mathrm{Li})_{\mathrm{NLTE}} = 2.16 \pm 0.16$. This is consistent with the Li abundance of unevolved metal-poor stars on the Spite plateau. The nearly constant level of Li in stars on the Spite plateau is only found for dwarfs and subgiants with $T_{\mathrm{eff}} \gtrsim 5700$ K, which is much warmer than the temperature of HKII 17435−00532 (e.g., Pilachowski et al. 1993; Ryan et al. 1996; Ryan & Deliyannis 1998). The Li enrichment mechanism of HKII 17435−00532 is likely unrelated to warm metal-poor turnoff stars, such as CS 22898−027 and LP 706-7. These stars have metallicities as low as or lower than HKII 17435−00532 and nearly identical Li abundances, yet they have (T_{eff}, log g) $\sim$ (6300 K, 4.0) and

(6000 K, 3.8), respectively (Thorburn & Beers 1992; Norris et al. 1997; Preston & Sneden 2001). The different evolutionary states of these stars indicate that different explanations for the Li enrichment may be necessary. High levels of Li have been observed in other evolved stars, too, but most of these stars have metallicities close to solar.

The surface ^{7}Li abundance in dwarf stars is depleted during main-sequence core H burning. This is because diffusion by gravitational settling becomes more efficient as the surface convection zone becomes increasingly shallow. Lower mass ($M \sim 0.5-0.65\ M_\odot$) stars have longer main-sequence lifetimes and also burn more ^{7}Li per unit time than higher mass ($M \sim 0.65-0.75\ M_\odot$) stars due to more effective convective mixing in their envelopes. Therefore, the lower mass main-sequence stars will exhibit more ^{7}Li depletion than higher mass main-sequence stars. As these stars evolve away from the main sequence, their convective zones deepen further, diluting the surface ^{7}Li abundance and destroying it in the deeper layers. More details of these processes are described in Deliyannis et al. (1990) and Proffitt & Michaud (1991).

Pilachowski et al. (1993) showed that Li abundances in metal-poor subgiants continue to decline by an additional factor of $\sim 10^1$–10^2 relative to the standard evolutionary model predictions as these stars ascend the RGB and AGB. Additional physical mechanisms, such as rotationally induced mixing, have been used to explain some of the observed ^{7}Li abundance decreases from predictions made from standard evolutionary models (see the discussion in, e.g., Pinsonneault et al. 1992; Deliyannis et al. 1993; Ryan & Deliyannis 1998). Even without detailed knowledge of the details of these processes, it is clear that the derived ^{7}Li abundance in HKII 17435−00532 cannot be its zero-age main-sequence ^{7}Li abundance.

There are several reasons to believe that the Li in HKII 17435−00532 was not transferred from an undetected companion. Our four radial velocity measurements for this star suggest that HKII 17435−00532 is not a member of a binary star system, although perhaps the system is a long-period binary or the plane of the orbit is nearly face-on with respect to the Earth. Even if HKII 17435−00532 is the secondary star of a binary system where the now unseen and presumably more massive primary swelled in size during its TP-AGB phase and transferred mass (including freshly synthesized Li) to the secondary, such a scenario would require extremely efficient mass transfer to enrich HKII 17435−00532 to $\log \varepsilon(\mathrm{Li}) \sim 2.1$.

Only two stars with $[\mathrm{Fe/H}] < -1.5$ have been reported to possess $\log \varepsilon(\mathrm{Li}) \gtrsim +2.4$: HD 160617 and BD +23 3912. While Charbonnel & Primas (2005) reported $\log \varepsilon(\mathrm{Li}) = +2.56$ in HD 160617, other studies have found lower abundances in this star, $\log \varepsilon(\mathrm{Li}) = +2.23$ (Pilachowski et al. 1993) and $\log \varepsilon(\mathrm{Li}) = +2.28$ (Asplund et al. 2006). Charbonnel & Primas (2005) also reported $\log \varepsilon(\mathrm{Li}) = +2.64$ in BD +23 3912, but other studies have also found lower abundances in this star, $\log \varepsilon(\mathrm{Li}) = +2.38$ (Pilachowski et al. 1993) and $\log \varepsilon(\mathrm{Li}) = +2.23$ (Thevenin 1998[18]).[19] Thus, it appears that Li enrichment significantly above the Spite plateau value in metal-poor stars is, at best, a rare phenomenon.

[18] Vizier Online Data Catalog, 3193 (F. Thevenin, 1998).

[19] We also note that neither of these subgiants exhibits any significant overabundances of C or Ba, two key signatures of *s*-process nucleosynthesis. In HD 160617, $[\mathrm{C/Fe}] = -0.6$ and $[\mathrm{Ba/Fe}] = 0.0$ (Jonsell et al. 2005; Johnson et al. 2007). In BD +23 3912, $[\mathrm{C/Fe}] = -0.2$ and $[\mathrm{Ba/Fe}] = +0.1$ (Fulbright 2000; Gratton et al. 2000).

Similarly, the lack of Li-enriched stars anywhere above the Spite plateau or the Li abundances expected by normal dilution as stars evolve up the RGB suggests that HKII 17435−00532 was not enriched during or prior to its departure from the main sequence, in which case it would be obeying the normal dilution effects predicted by standard evolutionary models. (In other words, the pattern of Li abundances seen in Fig. 4*b* of Ryan & Deliyannis 1998 has not been shifted upward by 1–2 dex due to extrinsic Li enrichment.)

Later, in § 7.3.2, we consider the possibility that the *n*-capture material in HKII 17435−00532 was accreted from a companion star that passed through the TP-AGB phase of evolution. In this scenario, we derive a dilution factor of 63 [where $\log_{10}(63) = 1.8$]; i.e., 1 part of accreted material is observable in the stellar atmosphere of HKII 17435−00532 for every 63 parts of its own, original material necessary to produce the observed *n*-capture abundances. If the Li shares its nucleosynthesis origin with this *n*-capture enrichment, it too would be expected to be diluted by the same factor. Figure 10 of Gratton et al. (2000) leads us to surmise that the unenriched Li abundance of HKII 17435−00532 would be $\log \varepsilon(\mathrm{Li}) \sim 0$–1 at its present evolutionary state. Therefore, in order to enrich HKII 17435−00532 to a present Li abundance of $\log \varepsilon(\mathrm{Li}) = +2.1$, nearly 3–4 dex (i.e., the sum of the enrichment and the logarithmic dilution factor) would need to be acquired by HKII 17435−00532 from its companion. Furthermore, the transfer would have needed to occur fairly recently; otherwise, the Li acquired by HKII 17435−00532 would be diluted and destroyed by the normal channels during its evolution up the RGB. The likelihood of such extreme enrichment seems small.

We conclude that the Li observed in HKII 17435−00532 is not of primordial origin and was not transferred from an unseen binary companion. The Li should have originated within this star.

6.2. CNO, α, and Fe Peak Elements

Carbon and oxygen are overabundant in HKII 17435−00532, with $[\mathrm{C/Fe}] \approx +0.7$ and $[\mathrm{O/Fe}] \approx +1.1$. The CN molecular band at 3850 Å commonly used to measure the N abundance was not covered in our spectra. Both McWilliam et al. (1995a, 1995b) and Cayrel et al. (2004) found a large amount of scatter in the C abundances of their very metal-poor star samples, despite the fact that the Cayrel et al. (2004) sample is biased against C-rich stars. It is difficult to ascertain whether the C overabundance in HKII 17435−00532 is typical for metal-poor stars or is the result of an additional enrichment process. If C enrichment has occurred, it is mild relative to the population of C-enriched metal-poor stars, which can have $[\mathrm{C/Fe}] \gtrsim 2.0$ in stars with similar metallicity to HKII 17435−00532 (Cohen et al. 2006; Aoki et al. 2007). Comparison of our O abundance with the O abundances of the sample of metal-poor subgiants and giants from García Pérez et al. (2006), both derived from the triplet near 7770 Å, reveals that the O abundance of HKII 17435−00532 is in very good agreement with their results. García Pérez et al. (2006) found $[\mathrm{O/Fe}] \sim +0.5$ near $[\mathrm{Fe/H}] = -2.2$ from the [O I] lines, which is only marginally smaller than our O abundance corrected for NLTE effects, and within the uncertainties of these measurements the HKII 17435−00532 O abundance is not anomalous. This suggests that no extra enrichment of O-rich material has occurred.

In Figure 4 we show the elemental abundances for $6 \leq Z \leq 30$ in HKII 17435−00532, the Sun, and 10 "typical" metal-poor stars. We represent the abundances of typical metal-poor stars by averaging the 10 most metal-rich ($-2.8 < [\mathrm{Fe/H}] < -2.0$) stars

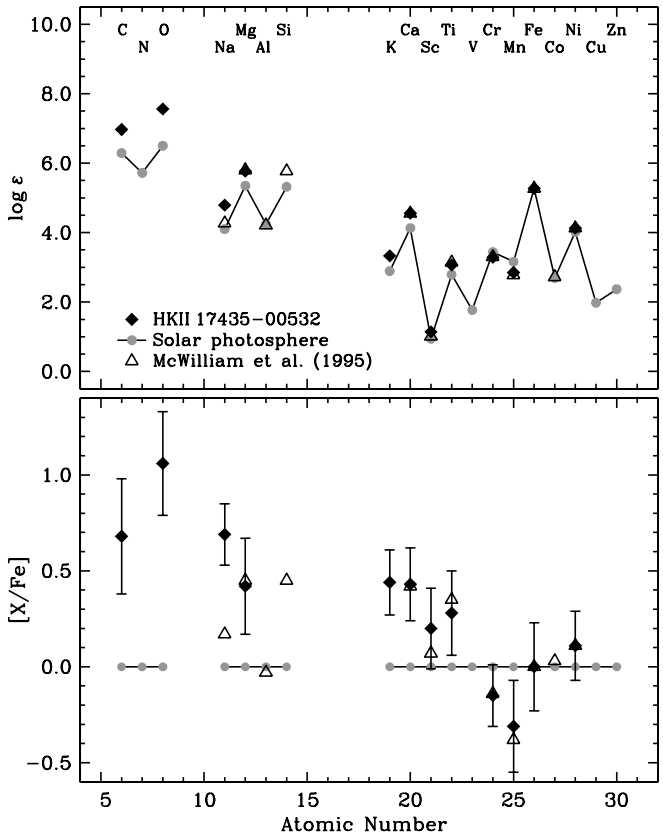

FIG. 4.—Light-element ($6 \leq Z \leq 30$) LTE abundances for HKII 17435−00532, the Sun, and "typical" metal-poor stars. The top panel shows absolute $\log \varepsilon$ abundances, and the bottom panel shows relative [X/Fe] abundances. We show the abundances for HKII 17435−00532 as filled diamonds. We also show the solar photospheric abundances as gray circles and connect them with a solid line. Open triangles represent "typical" metal-poor stars by averaging the 10 most metal-rich ($-2.8 < [\mathrm{Fe/H}] < -2.0$) stars in the McWilliam et al. (1995a, 1995b) sample. The abundances are normalized to the Fe abundance in HKII 17435−00532. [*See the electronic edition of the Journal for a color version of this figure*.]

in the McWilliam et al. (1995a, 1995b) sample. The well-known odd-even effect is clearly seen in the $\log \varepsilon$ abundances for these stars in Figure 4. With the exception of Na, the α and Fe peak elements appear very typical for a star in this metallicity regime.

Sodium is noticeably overabundant in HKII 17435−00532, $[\mathrm{Na/Fe}]_{\mathrm{LTE}} = +0.69$, although inclusion of NLTE effects for the $\lambda\lambda$5682 and 5688 Na lines could lower this abundance by $\sim$0.1 dex. Abundance analyses of large numbers of metal-poor stars (e.g., McWilliam et al. 1995a, 1995b; Cayrel et al. 2004) with $[\mathrm{Fe/H}] < -2.0$ have found little change in [Na/Fe] for metallicities $-3.0 < [\mathrm{Fe/H}] < -2.0$, with an intrinsic scatter of a few tenths of a dex. For the Pilachowski et al. (1996) field stars that have comparable temperature and gravity to HKII 17435−00532, we note that there exists a difference in their LTE Na abundances and the LTE Na abundance of HKII 17435−00532 by more than 0.4 dex, which presumably does represent a physical difference in the Na abundances and not, e.g., an effect of disregarding NLTE effects since the same set of Na lines were used for the analysis.

Gratton et al. (2000) found no evidence for a significant change in the Na abundance of field stars with $-2.0 < [\mathrm{Fe/H}] < -1.0$ along the RGB, although all of the stars in their sample exhibited $[\mathrm{Na/Fe}] \leq +0.4$. Aoki et al. (2007) also find a number of C-enriched metal-poor stars that have overabundances of Na, including some stars with $[\mathrm{Na/Fe}] > +2.0$. These authors showed that the Na enhancement in their sample correlated with C and

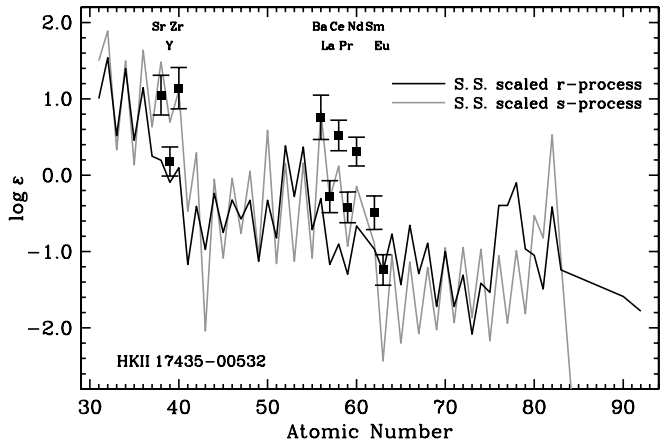

FIG. 5.—Derived abundances in HKII 17435−00532 and the scaled SS *s*- and *r*-process abundance patterns, indicated by the gray and black lines, respectively. The SS *s*-process distribution is normalized to Ba, and the SS *r*-process distribution is normalized to Eu. It is clear that neither distribution provides a satisfactory fit to the *n*-capture elemental abundance pattern in HKII 17435−00532. [*See the electronic edition of the Journal for a color version of this figure*.]

N enhancements. We note that the C and Na overabundances in HKII 17435−00532 are much less extreme than the C and Na overabundances in some of the stars in the Aoki et al. (2007) study. The available information hints that the Na overabundance in HKII 17435−00532 may share a common origin with the C overabundance rather than the evolutionary state of this star.

6.3. *n*-Capture Elements

HKII 17435−00532 exhibits overabundances of all *n*-capture elements relative to Fe when compared with the solar system (SS) abundance ratios. Both Ba and Eu exhibit significant overabundances in HKII 17435−00532, $[\mathrm{Ba/Fe}] = +0.86$ and $[\mathrm{Eu/Fe}] = +0.48$. These ratios suggest that HKII 17435−00532 is enriched to some degree in both *s*- and *r*-process material. Also, $[\mathrm{Ba/Eu}] = +0.38$, which suggests that the *s*-process has contributed a greater portion of the *n*-capture species in this star than the *r*-process. In Figure 5 we show the derived *n*-capture elemental abundances in HKII 17435−00532, as well as the scaled SS *s*- and *r*-process abundance patterns. If we examine the entire set of derived *n*-capture abundances in HKII 17435−00532, it is clear that the scaled solar abundances of neither process alone provide a satisfactory fit. Furthermore, within the ranges $38 \leq Z \leq 40$ and $56 \leq Z \leq 58$, the odd-even effect is more pronounced than would be expected, with the odd-*Z* elements exhibiting abundances $\sim$0.8–1.0 dex lower than the neighboring even-*Z* elements.

We display the abundance ratios for several sets of *n*-capture species in Figure 6 for HKII 17435−00532 and the 16 stars classified by Jonsell et al. (2006) as $(r + s)$-enriched.[20,21] The abundances of the *n*-capture species are all derived from transitions of singly ionized atoms, and the uncertainty in the surface gravity of the model atmosphere will have relatively small effects on the ratios of one *n*-capture species to another. Several of these ratios were chosen to examine whether the exaggerated *n*-capture odd-even-*Z* effect is common to other stars enriched in

[20] The star CS 31062−012 is also called LP 706-7 and has been listed twice in the Jonsell et al. (2006) table of $r + s$ stars. This double identification was also pointed out by Ryan et al. (2005).

[21] Strictly speaking, the Jonsell et al. (2006) $r + s$ classification refers to stars with $[\mathrm{Ba/Fe}] > +1.0$, $[\mathrm{Eu/Fe}] > +1.0$, and $[\mathrm{Ba/Eu}] > 0.0$, and HKII 17435−00532 does not meet these criteria. In this paper we refer to $r + s$ stars in a less strict sense to indicate that they exhibit some enhancement of both Ba and Eu, i.e., $+0.3 \lesssim [\mathrm{Ba/Fe}]$ and $+0.3 \lesssim [\mathrm{Eu/Fe}]$.

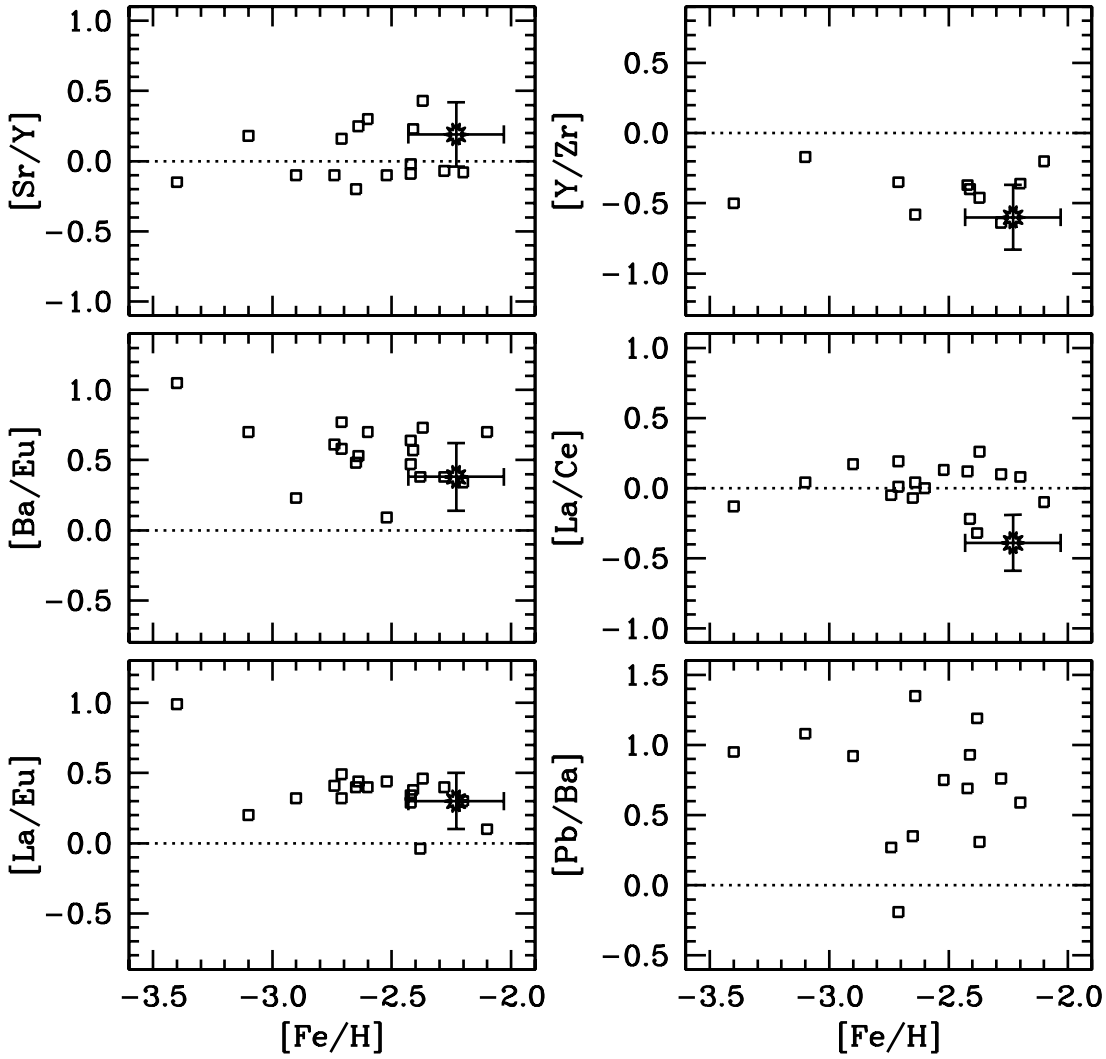

FIG. 6.—Abundance ratios of n-capture species for HKII 17435−00532 and other stars classified as $(r + s)$-enriched. HKII 17435−00532 is indicated by the sunburst, and other stars are indicated by open squares. The solar photospheric ratios are indicated by dotted lines. The additional data were taken from other studies and the $r + s$ list of Jonsell et al. (2006), which was compiled from the measurements of others, including Aoki et al. (2001, 2002), Barbuy et al. (2005), Barklem et al. (2005), Cohen et al. (2003, 2006), Hill et al. (2000), Ivans et al. (2005), Johnson & Bolte (2002, 2004), Lucatello et al. (2003), Masseron et al. (2006), Norris et al. (1997), Preston & Sneden (2001), and Sivarani et al. (2004). We also include the $r + s$ star CS 22964−161 (Thompson et al. 2008).

both s- and r-process material. In particular, the [Sr/Y] and [Y/Zr] ratios in HKII 17435−00532 appear normal with respect to other stars in this class. The [La/Ce] ratio is slightly lower in HKII 17435−00532 than the comparison stars but is still in agreement. The [Ba/Eu] and [La/Eu] ratios are in agreement. The [La/Eu] and [La/Ce] ratios exhibit remarkably small scatter among the stars of this class with the minor exceptions only for three stars. One of these stars, CS 29526−110, was noted by Aoki et al. (2002) to have a low La abundance. Jonsell et al. (2006) point out that HE 1405−0822 was noticed to have strong C molecular features in the spectrum by Barklem et al. (2005) and the data presented were preliminary. CS 30322−023, the most metal-poor star to demonstrate an s-process abundance signature, appears to have a rather low Eu abundance relative to the second s-process peak elements (Masseron et al. 2006). The exaggerated (relative to the scaled SS s- and r-process abundances) odd-even-Z effect for $38 \leq Z \leq 40$ and $56 \leq Z \leq 58$ appears to be a characteristic of the nucleosynthesis in these stars.

Despite the small intrinsic scatter among these abundance ratios, the scatter in the [Pb/Ba] ratio is noticeably greater, far beyond any reasonable variation in the atmospheric parameters or uncertainties in measuring the abundances of these stars (see also Masseron et al. 2006). No trend with [Fe/H] is apparent. It is likely that HKII 17435−00532 has an overabundance of Pb, but we do not presently know because our spectra do not include the Pb I λ4057 line to confirm this. For the often-discussed question of Ba and Pb abundances in the $(r + s)$-enriched stars we refer to Ivans et al. (2005), Bisterzo et al. (2006), and references therein.

We find a difference in the ratios of the mean light s-process abundances (Sr, Y, Zr; hereafter designated as ls) and heavy s-process abundances (Ba, La, Ce; hereafter designated as hs) to Fe, $[\mathrm{ls/Fe}] = 0.37 \pm 0.13$ and $[\mathrm{hs/Fe}] = 0.96 \pm 0.13$. In Figure 7 we show the [hs/ls] ratios for HKII 17435−00532 and other metal-poor stars as functions of [Ba/Eu] and [Fe/H]. Even though the Jonsell et al. (2006) $r + s$ classification required $[\mathrm{Ba/Fe}] > 1.0$ and $[\mathrm{Eu/Fe}] > 1.0$, greater than the [Ba/Fe] and [Eu/Fe] ratios in HKII 17435−00532, the [Ba/Eu] ratios for their stars are similar to ours. This suggests that HKII 17435−00532 may have less overall n-capture enrichment than the Jonsell et al. (2006) $r + s$ stars, but the relative amounts of enrichment may be similar. Also, HKII 17435−00532 and the $r + s$ stars fall in the

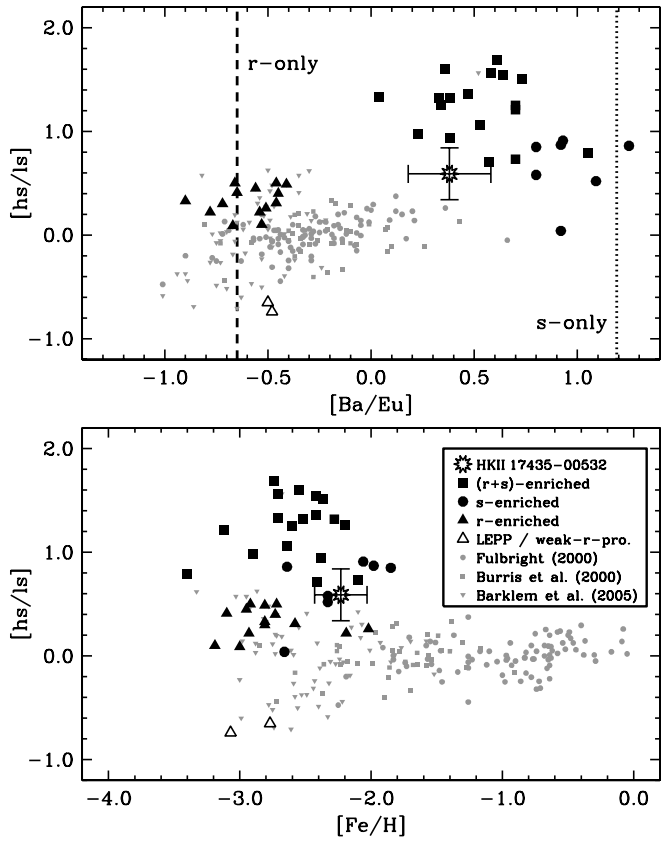

FIG. 7.—The [hs/ls] abundance ratio as a function of [Ba/Eu] (*top*) and [Fe/H] (*bottom*). HKII 17435−00532 is indicated by the sunburst. Large black squares, circles, and triangles indicate stars classified by Jonsell et al. (2006) as ($r + s$)-enriched, *s*-enriched, and *r*-enriched, respectively. Most of the Jonsell et al. (2006) classifications were based on measurements made by previous studies of these stars; we supplement their sample with HD 115444 (Westin et al. 2000), HD 221170 (Ivans et al. 2006), CS 30322−023 (Masseron et al. 2006), and CS 22964−161 (Thompson et al. 2008). Open triangles represent HD 122563 and HD 88609 (Honda et al. 2006, 2007), which may be enriched by products of the "Lighter Element Primary Process" (LEPP; Travaglio et al. 2004) or the weak *r*-process (Wanajo et al. 2006; Qian & Wasserburg 2007). Gray circles, squares, and triangles represent stars from the metal-poor abundance surveys of Fulbright (2000), Burris et al. (2000), and Barklem et al. (2005), respectively. The stellar model pure *s* and pure *r* [Ba/Eu] ratios (Arlandini et al. 1999) are shown by the dotted line and the dashed line, respectively. [*See the electronic edition of the Journal for a color version of this figure*.]

range between the pure *s* and pure *r* [Ba/Eu] ratios and between the stars classified as *s*-enriched and *r*-enriched. The [hs/ls] ratio in HKII 17435−00532 may lie between the [hs/ls] ratio in $r + s$- and *r*-enriched stars, but the uncertainties on this measurement are too great to clearly distinguish between these two classes.

From the data presented in Figure 7, it appears that, for the most part, stars enriched in both *s*- and *r*-process elements have high [hs/ls] ratios (i.e., [hs/ls] $\gtrsim 0.6$). Based on the overall chemical homogeneity of the stars in their $r + s$ class, Jonsell et al. (2006) argued that the *s*- and *r*-enrichment in these stars may not have originated from independent nucleosynthetic events. Furthermore, based on the frequency of $r + s$ stars in the HERES survey (Barklem et al. 2005) relative to the numbers of *r*-II and *s* stars, they concluded that the combination of *s*- and *r*-enrichment in the same star must point to a common (or at least a dependent set of) nucleosynthesis event(s).

Lucatello et al. (2006) have recently examined the C-rich and/or very cool stars, some of which include *n*-capture enhancements, that could not be studied by the automated procedures of Barklem et al. (2005). S. Lucatello et al. (2008, in preparation) are presently considering the frequency of the various categories of *n*-capture stars in the C-rich/cool sample, so we defer further discussion of such stars to their study. We also refer the reader to Bisterzo (2007) for a thorough comparison of chemical yields from stars in the TP-AGB phase to the *n*-capture abundances in $r + s$ stars.

Our Tc upper limit in HKII 17435−00532, $\log \varepsilon(\mathrm{Tc}) \lesssim +0.5$, is of little use, as it is 2–3 dex greater than the scaled *s*- and *r*-process predictions shown in Figure 5.

Given the metallicity of HKII 17435−00532, we can safely surmise that this star is very old ($\gtrsim$10 Gyr) and has a low mass ($\sim 0.8\,M_{\odot}$). The *s* and *r* nucleosynthesis reactions are not expected to operate in stars of such low mass, so they must have been present in the material from which this star formed or were transferred to it from an undetected binary companion.

TABLE 6
RADIAL VELOCITY VARIATIONS AMONG STARS EXHIBITING $r + s$ ENRICHMENT

Star Name	Radial Velocity Variations?[a]	Period (days)	References
HKII 17435−00532.....	N	...	1
CS 22183−015	Y	...	2, 3
CS 22898−027	N	...	4, 5
CS 22948−027	Y	426.5	5, 6
CS 22964−161	Y	252	7
CS 29497−030	Y	342	8, 9, 10
CS 29497−034	Y	4130	6
CS 29526−110	Y	...	4
CS 30322−023	N[b]	...	
CS 31062−012	N	...	11
CS 31062−050	Y	...	4, 12
HE 0024−2523.....	Y	3.41	13
HE 0131−3953.....	?	...	
HE 0338−3945.....	N	...	14
HE 1046−1352.....	?	...	
HE 1105+0027.....	?	...	
HE 1405−0822.....	?	...	
HE 2148−1247.....	Y	(Long)	15
LP 625-44	Y	$\gtrsim$4400	16

[a] A "Y" indicates that the star exhibits radial velocity variations, an "N" indicates that several measurements over a period of time have confirmed that the star does not exhibit radial velocity variations, and a "?" indicates that fewer than two radial velocity measurements have been reported in the literature.

[b] CS 30322−023 is in the TP-AGB phase and may exhibit a pulsation period of 192 days with an amplitude of $\approx$3 km s^{-1}. This may mask the detection of a long, low-amplitude orbital period, which cannot be ruled out by the available observations (Masseron et al. 2006).

REFERENCES.—(1) This study; (2) Cohen et al. 2006; (3) Lai et al. 2004; (4) Aoki et al. 2002; (5) Preston & Sneden 2001; (6) Barbuy et al. 2005; (7) Thompson et al. 2008; (8) Preston & Sneden 2000; (9) Sivarani et al. 2004; (10) Sneden et al. 2003; (11) Norris et al. 1997; (12) Aoki et al. 2003; (13) Lucatello et al. 2003; (14) Jonsell et al. 2006; (15) Cohen et al. 2003; (16) Aoki et al. 2000.

7. INTERPRETATION

We arrive at the challenge to find a consistent model to explain Li-, *s*-, and *r*-process enhancement, as well as C and Na enrichment, in a metal-poor star on the RGB, RHB, or early AGB. We have argued that the Li must have been produced in this star, while the *s*- and *r*-process elements must have been present in the material from which the star formed or were transferred to it by a nearby star. Radial velocity variations have not yet been detected, but we consider both binary and single-star explanations because of the possibility of a long binary orbital period or a highly inclined orbit.

In Table 6 we summarize the radial velocity measurements reported in the literature for HKII 17435−00532 and 18 other

$r + s$ stars. Of these 19 stars, 10 show clear evidence of radial velocity variations, 5 do not show any variations when observed for a substantial period of time (including HKII 17435−00532), and 4 have fewer than two measurements reported in the literature. Of the six stars with measured orbital periods, five have periods greater than 250 days, and one of these has a period greater than 12 yr. Given the similarities in the abundance ratios between these stars and HKII 17435−00532, as well as its unproven binary status, it is reasonable to expect that this star may be a long-period binary. Future radial velocity monitoring will be undertaken to investigate the matter. A wider binary separation could also explain the less extreme overabundances of *n*-capture material in HKII 17435−00532 relative to other $r + s$ stars, similar to the conclusion reached by Han et al. (1995) for the enrichment patterns in Ba and CH stars in binary systems. This explanation also gains support from the work of Lucatello et al. (2005), who observed radial velocity variations in 68% of their sample of 19 C- and *s*-process–enriched stars, yet were able to conclude from their Monte Carlo analysis of the sample that all C- and *s*-enriched metal-poor stars should be members of binary systems.

7.1. *Lithium Self-Enrichment through Extra Mixing*

7.1.1. *On the RGB*

The first dredge-up episode occurs on the lower RGB when the outer convective envelope deepens and encounters material that has been processed through H burning. Because it mixes fresh H from the surface downward into the star, the first dredge-up leaves a strong molecular weight discontinuity at the point of maximum penetration into the star. This material is outside of the H-burning shell, and when the H-burning shell burns outward through this molecular weight discontinuity, it encounters a fresh supply of H. As a result, the outward progress of the H-burning shell is halted, the radius of the star ceases to expand, and the star's ascent up the RGB is paused. The RGB luminosity bump occurs at the point on the RGB where stars spend a larger fraction of their time digesting this H fuel. The location of the RGB luminosity bump (which depends on metallicity), inferred from the calculations of Denissenkov & VandenBerg (2003), is indicated in Figure 1.

Before the H-burning shell erases the molecular weight discontinuity, no extra mixing can occur; after it has been erased, the star continues to evolve up the RGB. To explain the Li enrichment observed in some evolved stars, several authors (Charbonnel 1995; Sackmann & Boothroyd 1999; Charbonnel & Balachandran 2000) proposed that an extra, yet unspecified, mixing process may occur in low- and intermediate-mass stars (i.e., $1\ M_{\odot} \lesssim M \lesssim 5\ M_{\odot}$) after the molecular weight discontinuity has been erased at the RGB luminosity bump. The 3D simulations of the He flash presented in Dearborn et al. (2006) also suggest that this extra mixing may be present outside the H-burning shell. This extra mixing could drive ^{7}Li production by the Cameron & Fowler (1971) mechanism. This hypothesis explains the low- and intermediate-mass Li-enriched stars found at the RGB luminosity bump.

Once the H-burning shell begins to exhaust its fresh supply of H, it continues its outward burn, and the star once again expands and continues to ascend the RGB. The convective envelope extends deeper into the star, carrying the ^{7}Li to these hotter regions where it is destroyed. The Li-rich phase is fleeting. From the calculations presented in Denissenkov & Herwig (2004) for Li enrichment in low-mass, metal-poor stars along the RGB, we estimate that the Li-rich phase will not last more than 3–4 Myr.

What is the physical cause of the extra mixing process, and can it operate in low-mass, low-metallicity stars? Thermohaline mixing (Ulrich 1972; Kippenhahn et al. 1980; Eggleton et al. 2006, 2008) has long been considered plausible. This type of mixing is a result of a mean molecular weight inversion that arises in stars on the AGB when the ^{3}He(^{3}He, $2p$)^{4}He reaction lowers the mean molecular weight (from 3 to 2 for the species that participate in this reaction) near the upper boundary of the H-burning shell. Charbonnel & Zahn (2007) advocate a mechanism that relies on the double diffusion of both the mean molecular weight inversion and temperature instabilities to induce mixing. They successfully link changes in the surface ^{7}Li abundance (as well as a decrease in C and ^{12}C/^{13}C and an increase in N) to this extra mixing mechanism in low-mass ($M \sim 0.9\ M_{\odot}$), low-metallicity ([Fe/H] = −1.8, −1.3, −0.5) stars at and above the RGB luminosity bump.

Another possibility, known as the Li flash (Palacios et al. 2001), was found as a possible source of Li enrichment in solar-metallicity, $1.5\ M_{\odot}$ stars at the RGB luminosity bump. The creation of a thin Li-burning shell induces a convective instability, which carries Li to the surface of the star. The radius and luminosity of the star also increase, lifting the star off the RGB luminosity bump on the H-R diagram. If such a process could occur in low-mass, low-metallicity stars, this could also explain the Li enrichment observed in HKII 17435−00532.

If HKII 17435−00532 is ascending the RGB, the luminosity of this star is coincident with the luminosity of the bump for [Fe/H] = −2.2. It is possible that the present Li abundance has already been reduced from its maximum abundance. Since we cannot measure the ^{12}C/^{13}C ratio from our spectrum, we have no diagnostic tool to infer whether the surface Li abundance is still increasing, holding steady, or already decreasing. Such information would link the evolutionary status of HKII 17435−00532 with the apparent self-enrichment with Li: once the extra mixing extends deep enough to convert ^{12}C to ^{13}C, the hotter temperatures there will begin to destroy Li (Gratton et al. 2000; Spite et al. 2006). If HKII 17435−00532 is evolving through the RGB luminosity bump, it is the most metal-poor star for which an extra mixing mechanism has been shown to produce Li enrichment in the stellar envelope at this phase of evolution.

7.1.2. *On the RHB or Early AGB*

Enrichment of Li is not predicted to occur on the RHB or early AGB. Charbonnel & Balachandran (2000) note that an analog of the RGB extra mixing would have to be extremely efficient to connect the ^{3}He-rich envelope and the H-burning shell in lower mass, lower metallicity stars ascending the early AGB. The second dredge-up, which occurs after core He burning has ceased, does not affect the surface composition of stars with $M \lesssim 4\ M_{\odot}$ (Karakas et al. 2002). If our adopted surface gravity is too high and our adopted temperature is too cool, the star would still lie on the RHB or early AGB and, although we may have overestimated the mass of this star by $\sim$0.1–0.2 $M_{\odot}$, the Li question would remain.

We note that for stars in the later TP-AGB stage, H burning will alter the surface composition, including Li abundance, when the outer convective zone overlaps with the H-burning shell (hot bottom burning, or HBB; e.g., Sugimoto 1971; Forestini & Charbonnel 1997 and references therein) or when an extra mixing mechanism in the radiative layer above the H-burning shell connects it to the convective zone (cool bottom processing; e.g., Boothroyd et al. 1995; Wasserburg et al. 1995; Nollett et al. 2003 and references therein). These processes occur in higher luminosity stars [i.e., $\log (L/L_{\odot}) \gtrsim 3$], not lower luminosity stars

TABLE 7
Enhanced Na Abundances among Stars Exhibiting $r + s$ Enrichment

Star Name	$[Na/Fe]_{LTE}$	$[Na/Fe]_{NLTE}$	References
HKII 17435−00532	+0.69	+0.6	1
CS 22898−027	+0.17	...	2
CS 22948−027	+0.57	+0.07	3
CS 29497−030	+0.58	...	4
CS 29497−034	+1.18	+0.68	3
CS 30322−023	+1.29	...	5
CS 31062−012[a]	+1.3	+0.6	6

[a] CS 30322−023 = LP 706-7.

References.—(1) This study; (2) Preston & Sneden 2001; (3) Barbuy et al. 2005; (4) Ivans et al. 2005; (5) Masseron et al. 2006; (6) Aoki et al. 2007.

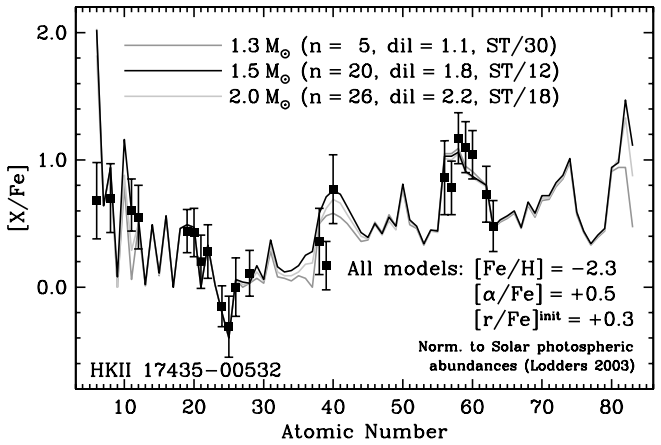

Fig. 8.—Predicted [X/Fe] ratios in HKII 17435−00532 assuming pollution from a companion star that passed through the TP-AGB phase. The abundance ratios have been normalized to the solar photospheric values given in Lodders (2003). LTE abundances are displayed for all elements except O, Na, and Mg, for which the NLTE-corrected abundances are displayed. The asymmetric uncertainties on Na reflect a conservative range on the NLTE corrections. All sets of abundance predictions assume $[Fe/H] = -2.3$, $[\alpha/Fe] = +0.5$, and $[r/Fe]^{init} = +0.3$. The initial mass of the TP-AGB star is the primary variable between the different sets of abundance predictions, although changing the mass necessitates altering the number of thermal pulses ("*n*"), the logarithmic dilution factor ("dil"), and the ^{13}C pocket efficiency ("ST/"). The black line reflects our best-fit model, with $M_{AGB} = 1.5\ M_{\odot}$, while the dark gray line and the light gray line have $M_{AGB} = 1.3$ and $2.0\ M_{\odot}$, respectively. [*See the electronic edition of the Journal for a color version of this figure.*]

near the base of the AGB (e.g., Kraft et al. 1999; Domínguez et al. 2004), and they are not suspects for the extra mixing in HKII 17435−00532. [Recall that $\log(L/L_{\odot}) \approx 2.0$ for HKII 17435−00532.]

If HKII 17435−00532 has recently arrived on the RHB from the tip of the RGB, is it possible that the supposed large Li overabundance that was produced by the Cameron & Fowler (1971) mechanism at the RGB luminosity bump has not yet been fully depleted? If we assume that the Li-rich phase will not last more than 3–4 Myr, this timescale is far shorter (by nearly 2 orders of magnitude) than the timescale necessary for the star to move from the RGB luminosity bump to the RHB (e.g., Campbell 2007, p. 252). We therefore dismiss this hypothesis.

Also, for metal-poor stars in globular clusters on the RGB or AGB, we note that Li production does not need to be associated with C, Na, *r*-process, or *s*-process enrichment (e.g., Kraft et al. 1999; Kraft & Shetrone 2000).

If HKII 17435−00532 is on the RHB or early AGB, we are left to postulate that a previously unidentified efficient extra mixing episode may be operating during this stage of evolution in low-mass, low-metallicity stars.

7.2. *Enhanced Sodium Abundance*

Several $r + s$ stars, including HKII 17435−00532, exhibit enhanced Na abundances, which we summarize in Table 7. ^{23}Na can be produced in thermally pulsing stars on the AGB through a series of reactions that convert CNO material produced during He burning into ^{23}Na. Briefly, as summarized by Sneden et al. (2008), the H-burning shell of an AGB star first converts CNO nuclei into ^{14}N. Then in the early phases of a thermal instability ^{22}Ne is generated in the α-capture reaction chain $^{14}N(\alpha,\gamma)^{18}F(\beta^{+}\nu)^{18}O(\alpha,\gamma)^{22}Ne$. Finally, enhanced ^{23}Na is produced by *n*-capture on the abundant ^{22}Ne and subsequent β^{-} decay. The available CNO nuclei include those present at the star's birth and fresh "primary" ^{12}C mixed into the envelope by previous third dredge-up (TDU) episodes. This primary source becomes predominant in very metal-poor AGB stars (e.g., Gallino et al. 2006). After the last TDU it is predicted that $[Na/Fe] \sim [Ne/Fe]$ (with Ne almost pure ^{22}Ne) in the AGB envelope.

7.3. *r + s Enrichment*

Unlike the case of Li enrichment, these scenarios are virtually independent of the evolutionary state, only assuming that this star is not in the TP-AGB stage.

7.3.1. *Preenrichment*

The simplest explanation assumes that HKII 17435−00532 is (and always has been) a single star. This scenario assumes that the material from which HKII 17435−00532 formed was enriched in both *s*- and *r*-process material and that no additional *n*-capture enrichment occurred. Evidence for *s*-process enrichment has been observed in a few stars with very low metallicities (e.g., CS 22183−015: $[Fe/H] = -3.1$, Johnson & Bolte 2002; CS 29497−030: $[Fe/H] = -2.8$, Sivarani et al. 2004; CS 30322−023: $[Fe/H] = -3.4$, Masseron et al. 2006), and *r*-process material has been found in stars of all metallicities (at least for those with $[Fe/H] \gtrsim -4.0$). In a generation of stars that preceded HKII 17435−00532, it is possible that at least one binary pair formed with one star that would ultimately explode as a supernova, producing *r*-process material, and another star that would ultimately produce *s*-process material during its TP-AGB phase. This *s*- and *r*-enriched material would then be recycled into the interstellar medium (ISM) from which HKII 17435−00532 later formed. Such a scenario cannot be ruled out and would also account for the possible link between the *s*- and *r*-enrichment mechanisms.

7.3.2. *Pollution from a 1.5 $M_{\odot}$ Companion*

Let us assume the binary scenario for HKII 17435−00532, in which we consider the observed star to be the longer lived secondary. We calculate the *s*-process yields from the primary, assuming that both members of the binary had the same initial metallicity. These calculations were based on the FRANEC stellar evolution models (Straniero et al. 1997, 2003; Zinner et al. 2006) for low-metallicity stars on the AGB. The best fit is obtained with the model that adopts an initial mass of $1.5\ M_{\odot}$ for the companion star that passed through the TP-AGB phase. Abundance predictions for three sets of model parameters are displayed in Figure 8. The initial mass of the companion star is the independent variable, although changing the mass affects the number of *s*-process–producing thermal pulses ("*n*") that occur, the logarithmic dilution factor ("dil"; defined to be the logarithm of the ratio of original mass in the observed stellar

envelope to the amount of mass that is acquired), and the ^{13}C pocket efficiency ("ST/"; i.e., some fraction of the standard ^{13}C pocket efficiency of Gallino et al. 1998). As basic model input, we adopt $[\mathrm{Fe/H}] = -2.3$, $[\alpha/\mathrm{Fe}] = +0.5$, and $[r/\mathrm{Fe}]^{\mathrm{init}} = +0.3$.

If we adopt the various Na NLTE corrections for the $\lambda\lambda$5682 and 5688 lines at face value, a conservative range for the Na abundance is found to be $0.45 < [\mathrm{Na/Fe}] < 0.85$. This constrains the mass of the undetected companion to $1.3\ M_{\odot} \lesssim M \lesssim 2.0\ M_{\odot}$. Of the elemental abundances we have measured in HKII 17435−00532, the Na abundance is the best discriminator of the mass of the companion star. The α and Fe peak abundance ratios are insensitive to the model parameters.

We derive a dilution factor of 1.8 dex (i.e., a factor of ≈63) for this system, assuming that the companion had a main-sequence mass of 1.5 $M_{\odot}$. An initial enrichment of *r*-process material is assumed in these models, but Eu is the only species that we measure in HKII 17435−00532 that is strongly sensitive to this enrichment. If we assume an initial $[r/\mathrm{Fe}] = +0.3$ for this system, then only ∼0.2 dex of Eu needs to be acquired from the *s*-process material of the AGB companion. In contrast to the Eu, which mostly reflects the initial composition of the ISM from which the system formed, the Ba (and other hs species with large overabundances) was dominantly produced by the companion star during its TP-AGB phase and transferred to HKII 17435−00532 by *s*-process–enriched winds.

Predictions for the abundances of *n*-capture species vary somewhat depending on the parameter choices, but they generally agree with the observations. The most notable exception is Y, which is predicted to be overabundant by roughly +0.5−0.7 dex but is measured to have $[\mathrm{Y/Fe}] = +0.17 \pm 0.19$. Similar results were found by Aoki et al. (2006) for CS 31062−050 and LP 625-44. If we were to adopt initial enrichment levels for Sr, Y, and Zr from the distribution of unevolved stars compiled by Travaglio et al. (2004), $[\mathrm{Sr/Fe}] = +0.2$, $[\mathrm{Y/Fe}] = -0.2$, and $[\mathrm{Zr/Fe}] = +0.4$, the changes in the final abundance predictions for [Y/Fe] are only decreased by ≈0.1 dex, while the predicted [Sr/Fe] and [Zr/Fe] ratios remain approximately unchanged.

7.3.3. *Enrichment from an 8–10 $M_{\odot}$ Companion*

Another enrichment scenario invokes a single high-mass companion star as the donor of both the *s*- and *r*-process material to HKII 17435−00532. Type II supernovae with $8.0\ M_{\odot} \lesssim M \lesssim 10.0\ M_{\odot}$ have been identified as a possible source of *r*-process elements (specifically, Eu) in low-metallicity stars (Mathews et al. 1992; Ishimaru & Wanajo 1999; Wanajo et al. 2003; Ishimaru et al. 2004; Ning et al. 2007). Similarly, at progressively lower metallicities, stars with smaller initial masses will end the AGB phase of their life with masses above the Chandrasekhar limit and may explode as Type 1.5 (or AGB) supernovae and produce *r*-process material (Iben & Renzini 1983; Zijlstra 2004). It has been shown (e.g., Gallino et al. 1998; Busso et al. 1999) that the main component of the *s*-process occurs during the interpulse phases of intermediate-mass stars on the AGB ($1.5\ M_{\odot} < M < 3.0\ M_{\odot}$). Due to the accelerated evolutionary rates of stars with $M > 3.0\ M_{\odot}$ and the relatively small amount of mass located in the intershell region, however, very small amounts of *s*-process material are expected to be produced by TP-AGB stars in the $8.0\ M_{\odot} \lesssim M \lesssim 10.0\ M_{\odot}$ range. Consequently, we dismiss this unlikely enrichment scenario for HKII 17435−00532.

7.3.4. *Enrichment from Two Companion Stars*

A long-period triple-star system could be invoked to explain *r*-process material from a high-mass ($M \gtrsim 8\ M_{\odot}$) supernova and *s*-process material from an intermediate-mass ($1.5\ M_{\odot} \lesssim M \lesssim 3.0\ M_{\odot}$) star on the AGB, both of which deposited some of this *n*-capture–enriched material on the tertiary star. In the case that such a system is dynamically stable for the length of the lifetime of a high-mass star, the object could evolve, explode as a supernova, and enrich the two remaining stars with *r*-process material. If the two remaining stars then became separated from the compact supernova remnant but remained gravitationally bound, the intermediate-mass star could evolve, pass through the TP-AGB phase, and transfer *s*-process–enriched material to the low-mass tertiary. The very large orbital separation that would be necessary to maintain the triple system for a long period of time would necessarily imply a large dilution of the transferred material. Although perhaps a less likely scenario than the single 1.5 $M_{\odot}$ AGB companion scenario, the triple-star system nevertheless could account for the *n*-capture enrichment pattern observed in HKII 17435−00532.

8. CONCLUSIONS

We have performed the first detailed abundance analysis on HKII 17435−00532, a star that was identified as a metal-poor candidate during the original HK survey and reidentified during the HK-II survey. High-resolution spectra necessary for this abundance analysis were obtained with the HRS on the HET at McDonald Observatory. No radial velocity variations are detected over a time span of ∼180 days, which prevents us from distinguishing whether HKII 17435−00532 is a single star, a member of a long-period binary system, or in a binary system with a highly inclined orbit. Future radial velocity monitoring may shed light on the situation. We derive $T_{\mathrm{eff}} = 5200 \pm 150$ K and $\log g = 2.15 \pm 0.4$ for HKII 17435−00532, which places it on the RGB or the RHB/early AGB. Our abundance analysis reveals that this star is indeed metal-poor, with $[\mathrm{Fe/H}] = -2.2$.

A surprising result of our study is the high Li abundance, $\log \varepsilon(\mathrm{Li}) = +2.1$, which is not predicted by standard stellar models for a low-mass, low-metallicity, evolved star such as HKII 17435−00532. If this star is evolving up the RGB, it is located near the RGB luminosity bump, where extra mixing has been found to cause a short-lived phase of Li enrichment in more massive stars. In this case, HKII 17435−00532 would represent the most metal-poor object known for which this extra mixing phenomenon occurs. If the star is on the RHB or early AGB, any Li that was present at earlier times should have been destroyed. In this case, we propose that an analog of the extra mixing that occurs at the RGB luminosity bump may be occurring on the RHB/early AGB. Future theoretical analysis of this point would be necessary to confirm or refute this hypothesis. Measurement of the ^{12}C/^{13}C ratio would also help to better constrain the evolutionary state of this star.

Our abundance analysis also finds that C and Na are slightly enhanced. The abundances of O, the α-elements, and the Fe peak elements all appear typical for stars with metallicity similar to HKII 17435−00532. This star is enriched with both *s*- and *r*-process elements. Several scenarios can be invoked to explain the *n*-capture abundance patterns, as well as the C and Na enhancements. These include preenrichment from supernovae, mass transfer from a companion in the TP-AGB phase, or enrichment from a nearby supernova. Our favored scenario involves pollution from a binary companion star with an initial mass of ≈1.5 $M_{\odot}$; this would only require that a small initial enrichment of *r*-process material was present in the ISM from which this star formed.

Inefficient mixing of the ISM, differing efficiencies of stellar winds from stars on the AGB, or a wide range of orbital separations can likely account for the range of C, Na, *s*-process, and *r*-process enrichments observed in $r + s$ stars. Future studies of

the frequency, binarity, and abundance patterns of stars enriched in both *s*- and *r*-process material will be necessary to understand the origins of this class of stars.

We gratefully thank Amanda Karakas and Oscar Straniero for enlightening discussions and the referee for providing a helpful set of constructive suggestions on the manuscript. We also acknowledge Yoichi Takeda for sharing his *K* NLTE correction interpolation routine, Eusebio Terrazas and Frank Deglman for their support of these HET observations, and Joy Chavez for taking one of the epochs of the 2.7 m data. We are indebted to Taylor Chonis and Martin Gaskell for obtaining new photometry of HKII 17435−00532 from the Miller Observatory. The Hobby-Eberly Telescope (HET) is a joint project of the University of Texas at Austin, Pennsylvania State University, Stanford University, Ludwig-Maximilians-Universität München, and Georg-August-Universität Göttingen. The HET is named in honor of its principal benefactors, William P. Hobby and Robert E. Eberly. This research has made use of the NASA Astrophysics Data System (ADS), NIST Atomic Spectra Database, The Amateur Sky Survey (TASS), Two Micron All-Sky Survey (2MASS), and SIMBAD databases. The reliability and accessibility of these online databases are greatly appreciated. A. F. acknowledges support through the W. J. McDonald Fellowship of the McDonald Observatory. J. R. gratefully acknowledges partial research support for this work by NASA through the AAS Small Research Grant Program and the *GALEX* GI grant 05-GALEX05-27. R. G. acknowledges the Italian MIUR-PRIN06 Project "Late Phases of Stellar Evolution: Nucleosynthesis in Supernovae, AGB Stars, Planetary Nebulae" for support. Funding for this project has also been generously provided by the US National Science Foundation (grant AST 06-07708 to C. S; grants AST 04-06784, AST 07-07776, and PHY 02-15783 to T. C. B. and the Physics Frontier Center/Joint Institute for Nuclear Astrophysics [JINA]; and grant AST 07-07447 to J. J. C.).

REFERENCES

Allende Prieto, C., et al. 2008, AJ, submitted
Alonso, A., Arribas, S., & Martínez-Roger, C. 1996, A&A, 313, 873
———. 1999, A&AS, 140, 261
Aoki, W., Beers, T. C., Christlieb, N., Norris, J. E., Ryan, S. G., & Tsangarides, S. 2007, ApJ, 655, 492
Aoki, W., Bisterzo, S., Gallino, R., Beers, T. C., Norris, J. E., Ryan, S. G., & Tsangarides, S. 2006, ApJ, 650, L127
Aoki, W., Norris, J. E., Ryan, S. G., Beers, T. C., & Ando, H. 2000, ApJ, 536, L97
Aoki, W., Ryan, S. G., Norris, J. E., Beers, T. C., Ando, H., & Tsangarides, S. 2002, ApJ, 580, 1149
Aoki, W., et al. 2001, ApJ, 561, 346
———. 2003, ApJ, 592, L67
———. 2005, ApJ, 632, 611
Arlandini, C., Käppeler, F., Wisshak, K., Gallino, R., Lugaro, M., Busso, M., & Straniero, O. 1999, ApJ, 525, 886
Asplund, M. 2005, ARA&A, 43, 481
Asplund, M., Grevesse, N., & Sauval, A. J. 2005, in ASP Conf. Ser. 336, Cosmic Abundances as Records of Stellar Evolution and Nucleosynthesis, ed. T. G. Barnes III & F. N. Bash (San Francisco: ASP), 25
Asplund, M., Lambert, D. L., Nissen, P. E., Primas, F., & Smith, V. V. 2006, ApJ, 644, 229
Barbuy, B., Spite, M., Spite, F., Hill, V., Cayrel, R., Plez, B., & Petitjean, P. 2005, A&A, 429, 1031
Barbuy, B., et al. 2003, ApJ, 588, 1072
Barklem, P. S., et al. 2005, A&A, 439, 129
Beers, T. C., Preston, G. W., & Shectman, S. A. 1985, AJ, 90, 2089
———. 1992, AJ, 103, 1987
Behr, B. B. 2003, ApJS, 149, 101
Bihain, G., Israelian, G., Rebolo, R., Bonifacio, P., & Molaro, P. 2004, A&A, 423, 777
Bisterzo, S. 2007, Ph.D. thesis, Univ. Torino
Bisterzo, S., Gallino, R., Straniero, O., Ivans, I. I., Käppeler, F., & Aoki, W. 2006, Mem. Soc. Astron. Italiana, 77, 985
Bonifacio, P., et al. 2007, A&A, 462, 851
Boothroyd, A. I., Sackmann, I.-J., & Wasserburg, G. J. 1995, ApJ, 442, L21
Bruls, J. H. M. J., Rutten, R. J., & Shchukina, N. G. 1992, A&A, 265, 237
Burris, D. L., Pilachowski, C. A., Armandroff, T. E., Sneden, C., Cowan, J. J., & Roe, H. 2000, ApJ, 544, 302
Burstein, D., & Heiles, C. 1982, AJ, 87, 1165
Busso, M., Gallino, R., & Wasserburg, G. J. 1999, ARA&A, 37, 239
Cameron, A. G. W. 1955, ApJ, 121, 144
Cameron, A. G. W., & Fowler, W. A. 1971, ApJ, 164, 111
Campbell, S. W. 2007, Ph.D. thesis, Monash Univ.
Carlsson, M., Rutten, R. J., Bruls, J. H. M. J., & Shchukina, N. G. 1994, A&A, 288, 860
Carollo, D., et al. 2007, Nature, 450, 1020
Cassisi, S., Castellani, M., Caputo, F., & Castellani, V. 2004, A&A, 426, 641
Cavallo, R. M., Pilachowski, C. A., & Rebolo, R. 1997, PASP, 109, 226
Cayrel, R., et al. 2004, A&A, 416, 1117
Charbonnel, C. 1995, ApJ, 453, L41
Charbonnel, C., & Balachandran, S. C. 2000, A&A, 359, 563
Charbonnel, C., & Primas, F. 2005, A&A, 442, 961
Charbonnel, C., & Zahn, J.-P. 2007, A&A, 467, L15
Clayton, D. D., Fowler, W. A., Hull, T. E., & Zimmermann, B. A. 1961, Ann. Phys., 12, 331
Cohen, J. G., Christlieb, N., Qian, Y.-Z., & Wasserburg, G. J. 2003, ApJ, 588, 1082
Cohen, J. G., et al. 2006, AJ, 132, 137
Dearborn, D. S. P., Lattanzio, J. C., & Eggleton, P. P. 2006, ApJ, 639, 405
Deliyannis, C. P., Demarque, P., & Cavalier, S. D. 1990, ApJS, 73, 21
Deliyannis, C. P., Pinsonneault, M. H., & Duncan, D. K. 1993, ApJ, 414, 740
Demarque, P., Woo, J.-H., Kim, Y.-C., & Yi, S. K. 2004, ApJS, 155, 667
Denissenkov, P. A., & Herwig, F. 2004, ApJ, 612, 1081
Denissenkov, P. A., & VandenBerg, D. A. 2003, ApJ, 593, 509
Domínguez, I., Abia, C., Straniero, O., Cristallo, S., & Pavlenko, Y. V. 2004, A&A, 422, 1045
Droege, T. F., Richmond, M. W., Sallman, M. P., & Creager, R. P. 2006, PASP, 118, 1666
Eggleton, P. P., Dearborn, D. S. P., & Lattanzio, J. C. 2006, Science, 314, 1580
———. 2008, ApJ, 677, 581
Fitzpatrick, M. J., & Sneden, C. 1987, BAAS, 19, 1129
Forestini, M., & Charbonnel, C. 1997, A&AS, 123, 241
Frebel, A., Norris, J. E., Aoki, W., Honda, S., Bessell, M. S., Takada-Hidai, M., Beers, T. C., & Christlieb, N. 2007, ApJ, 658, 534
Fulbright, J. P. 2000, AJ, 120, 1841
Fulbright, J. P., & Johnson, J. A. 2003, ApJ, 595, 1154
Gallino, R., Arlandini, C., Busso, M., Lugaro, M., Travaglio, C., Straniero, O., Chieffi, A., & Limongi, M. 1998, ApJ, 497, 388
Gallino, R., Bisterzo, S., Straniero, O., Ivans, I. I., & Käppeler, F. 2006, Mem. Soc. Astron. Italiana, 77, 786
García Pérez, A. E., Asplund, M., Primas, F., Nissen, P. E., & Gustafsson, B. 2006, A&A, 451, 621
Gehren, T., Liang, Y. C., Shi, J. R., Zhang, H. W., & Zhao, G. 2004, A&A, 413, 1045
Gratton, R. G., Carretta, E., Claudi, R., Lucatello, S., & Barbieri, M. 2003, A&A, 404, 187
Gratton, R. G., Carretta, E., Eriksson, K., & Gustafsson, B. 1999, A&A, 350, 955
Gratton, R. G., Sneden, C., Carretta, E., & Bragaglia, A. 2000, A&A, 354, 169
Grevesse, N., & Sauval, A. J. 2002, Adv. Space Res., 30, 3
Han, Z., Eggleton, P. P., Podsiadlowski, P., & Tout, C. A. 1995, MNRAS, 277, 1443
Hill, V., et al. 2000, A&A, 353, 557
Hinkle, K., Wallace, L., Valenti, J., & Harmer, D., eds. 2000, Visible and Near Infrared Atlas of the Arcturus Spectrum 3727–9300 Å (San Francisco: ASP)
Hobbs, L. M., Thorburn, J. A., & Rebull, L. M. 1999, ApJ, 523, 797
Honda, S., Aoki, W., Ishimaru, Y., & Wanajo, S. 2007, ApJ, 666, 1189
Honda, S., Aoki, W., Ishimaru, Y., Wanajo, S., & Ryan, S. G. 2006, ApJ, 643, 1180
Honda, S., Aoki, W., Kajino, T., Ando, H., Beers, T. C., Izumiura, H., Sadakane, K., & Takada-Hidai, M. 2004a, ApJ, 607, 474
Honda, S., et al. 2004b, ApJS, 152, 113
Iben, I., Jr., & Renzini, A. 1983, ARA&A, 21, 271
Ishimaru, Y., & Wanajo, S. 1999, ApJ, 511, L33
Ishimaru, Y., Wanajo, S., Aoki, W., & Ryan, S. G. 2004, ApJ, 600, L47

Ivans, I. I., Simmerer, J., Sneden, C., Lawler, J. E., Cowan, J. J., Gallino, R., & Bisterzo, S. 2006, ApJ, 645, 613
Ivans, I. I., Sneden, C., Gallino, R., Cowan, J. J., & Preston, G. W. 2005, ApJ, 627, L145
Ivarsson, S., Litzén, U., & Wahlgren, G. M. 2001, Phys. Scr., 64, 455
Johnson, J. A. 2002, ApJS, 139, 219
Johnson, J. A., & Bolte, M. 2002, ApJ, 579, L87
———. 2004, ApJ, 605, 462
Johnson, J. A., Herwig, F., Beers, T. C., & Christlieb, N. 2007, ApJ, 658, 1203
Jonsell, K., Barklem, P. S., Gustafsson, B., Christlieb, N., Hill, V., Beers, T. C., & Holmberg, J. 2006, A&A, 451, 651
Jonsell, K., Edvardsson, B., Gustafsson, B., Magain, P., Nissen, P. E., & Asplund, M. 2005, A&A, 440, 321
Käppeler, F., Beer, H., & Wisshak, K. 1989, Rep. Prog. Phys., 52, 945
Karakas, A. I., Lattanzio, J. C., & Pols, O. R. 2002, Publ. Astron. Soc. Australia, 19, 515
Kim, Y.-C., Demarque, P., Yi, S. K., & Alexander, D. R. 2002, ApJS, 143, 499
Kippenhahn, R., Ruschenplatt, G., & Thomas, H.-C. 1980, A&A, 91, 175
Kiselman, D. 2001, NewA Rev., 45, 559
Korn, A. J., Grundahl, F., Richard, O., Barklem, P. S., Mashonkina, L., Collet, R., Piskunov, N., & Gustafsson, B. 2006, Nature, 442, 657
Kraft, R. P., Peterson, R. C., Guhathakurta, P., Sneden, C., Fulbright, J. P., & Langer, G. E. 1999, ApJ, 518, L53
Kraft, R. P., & Shetrone, M. D. 2000, in The Galactic Halo: From Globular Cluster to Field Stars, ed. A. Noels et al. (Belgium: Institut d'Astrophysique et de Geophysique), 177
Kurucz, R. L. 1993, Kurucz CD-ROM 13, ATLAS 9 Stellar Atmosphere Programs and 2 km/s Grid (Cambridge: SAO)
Lai, D. K., Bolte, M., Johnson, J. A., & Lucatello, S. 2004, AJ, 128, 2402
Lawler, J. E., Bonvallet, G., & Sneden, C. 2001a, ApJ, 556, 452
Lawler, J. E., Wickliffe, M. E., den Hartog, E. A., & Sneden, C. 2001b, ApJ, 563, 1075
Lodders, K. 2003, ApJ, 591, 1220
Lucatello, S., Beers, T. C., Christlieb, N., Barklem, P. S., Rossi, S., Marsteller, B., Sivarani, T., & Lee, Y. S. 2006, ApJ, 652, L37
Lucatello, S., Gratton, R., Cohen, J. G., Beers, T. C., Christlieb, N., Carretta, E., & Ramírez, S. 2003, AJ, 125, 875
Lucatello, S., Tsangarides, S., Beers, T. C., Carretta, E., Gratton, R. G., & Ryan, S. G. 2005, ApJ, 625, 825
Masseron, T., et al. 2006, A&A, 455, 1059
Mathews, G. J., Bazan, G., & Cowan, J. J. 1992, ApJ, 391, 719
McWilliam, A. 1998, AJ, 115, 1640
McWilliam, A., Preston, G. W., Sneden, C., & Searle, L. 1995a, AJ, 109, 2757
McWilliam, A., Preston, G. W., Sneden, C., & Shectman, S. 1995b, AJ, 109, 2736
Meléndez, J., & Ramírez, I. 2004, ApJ, 615, L33
Mendez, R. A., & van Altena, W. F. 1998, A&A, 330, 910
Mishenina, T. V., & Kovtyukh, V. V. 2001, A&A, 370, 951
Munari, U., & Zwitter, T. 1997, A&A, 318, 269
Ning, H., Qian, Y.-Z., & Meyer, B. S. 2007, ApJ, 667, L159
Nissen, P. E., Akerman, C., Asplund, M., Fabbian, D., Kerber, F., Kaufl, H. U., & Pettini, M. 2007, A&A, 469, 319
Nissen, P. E., Primas, F., Asplund, M., & Lambert, D. L. 2002, A&A, 390, 235
Nollett, K. M., Busso, M., & Wasserburg, G. J. 2003, ApJ, 582, 1036
Norris, J. E., Ryan, S. G., & Beers, T. C. 1997, ApJ, 488, 350
Palacios, A., Charbonnel, C., & Forestini, M. 2001, A&A, 375, L9
Piau, L., Beers, T. C., Balsara, D. S., Sivarani, T., Truran, J. W., & Ferguson, J. W. 2006, ApJ, 653, 300
Pilachowski, C. A., Sneden, C., & Booth, J. 1993, ApJ, 407, 699
Pilachowski, C. A., Sneden, C., & Kraft, R. P. 1996, AJ, 111, 1689
Pinsonneault, M. H., Deliyannis, C. P., & Demarque, P. 1992, ApJS, 78, 179
Piskunov, N. E., & Valenti, J. A. 2002, A&A, 385, 1095
Preston, G. W., & Sneden, C. 2000, AJ, 120, 1014
———. 2001, AJ, 122, 1545
Preston, G. W., Sneden, C., Thompson, I. B., Shectman, S. A., & Burley, G. S. 2006, AJ, 132, 85
Proffitt, C. R., & Michaud, G. 1991, ApJ, 380, 238
Qian, Y.-Z., & Wasserburg, G. J. 2007, Phys. Rep., 442, 237
Ramírez, I., & Meléndez, J. 2005a, ApJ, 626, 446
———. 2005b, ApJ, 626, 465
Ramsey, L. W., et al. 1998, Proc. SPIE, 3352, 34
Reddy, B. E., & Lambert, D. L. 2005, AJ, 129, 2831
Rhee, J. 2001, PASP, 113, 1569
Roederer, I. U., Lawler, J. E., Sneden, C., Cowan, J. J., Sobeck, J. S., & Pilachowski, C. A. 2008, ApJ, 675, 723
Ryan, S. G., Aoki, W., Norris, J. E., & Beers, T. C. 2005, ApJ, 635, 349
Ryan, S. G., Beers, T. C., Deliyannis, C. P., & Thorburn, J. A. 1996, ApJ, 458, 543
Ryan, S. G., & Deliyannis, C. P. 1998, ApJ, 500, 398
Sackmann, I.-J., & Boothroyd, A. I. 1999, ApJ, 510, 217
Salaris, M., Chieffi, A., & Straniero, O. 1993, ApJ, 414, 580
Sansonetti, C. J., Richou, B., Engleman, R. J., & Radziemski, L. J. 1995, Phys. Rev. A, 52, 2682
Schlegel, D. J., Finkbeiner, D. P., & Davis, M. 1998, ApJ, 500, 525
Seeger, P. A., Fowler, W. A., & Clayton, D. D. 1965, ApJS, 11, 121
Shetrone, M., et al. 2007, PASP, 119, 556
Simmerer, J., Sneden, C., Cowan, J. J., Collier, J., Woolf, V. M., & Lawler, J. E. 2004, ApJ, 617, 1091
Sivarani, T., et al. 2004, A&A, 413, 1073
Skrutskie, M. F., et al. 2006, AJ, 131, 1163
Smith, V. V., Lambert, D. L., & Nissen, P. E. 1993, ApJ, 408, 262
Sneden, C., Cowan, J. J., & Gallino, R. 2008, ARA&A, in press
Sneden, C., Preston, G. W., & Cowan, J. J. 2003, ApJ, 592, 504
Sneden, C. A. 1973, Ph.D. thesis, Univ. Texas at Austin
Sobeck, J. S., Lawler, J. E., & Sneden, C. 2007, ApJ, 667, 1267
Spergel, D. N., et al. 2007, ApJS, 170, 377
Spite, F., & Spite, M. 1982, A&A, 115, 357
Spite, M., et al. 2006, A&A, 455, 291
Straniero, O., Chieffi, A., Limongi, M., Busso, M., Gallino, R., & Arlandini, C. 1997, ApJ, 478, 332
Straniero, O., Domínguez, I., Cristallo, R., & Gallino, R. 2003, Publ. Astron. Soc. Australia, 20, 389
Sugimoto, D. 1971, Prog. Theor. Phys., 45, 761
Takada-Hidai, M., Saito, Y.-J., Takeda, Y., Honda, S., Sadakane, K., Masuda, S., & Izumiura, H. 2005, PASJ, 57, 347
Takeda, Y., Zhao, G., Chen, Y.-Q., Qiu, H.-M., & Takada-Hidai, M. 2002, PASJ, 54, 275
Takeda, Y., Zhao, G., Takada-Hidai, M., Chen, Y.-Q., Saito, Y.-J., & Zhang, H.-W. 2003, Chinese J. Astron. Astrophys., 3, 316
Thevenin, F. 1998, Bull. Cent. Donnees Stellaires, 49
Thompson, I. B., et al. 2008, ApJ, 677, 556
Thorburn, J. A., & Beers, T. C. 1992, BAAS, 24, 1278
Travaglio, C., Gallino, R., Arnone, E., Cowan, J., Jordan, F., & Sneden, C. 2004, ApJ, 601, 864
Tull, R. G. 1998, Proc. SPIE, 3355, 387
Tull, R. G., MacQueen, P. J., Sneden, C., & Lambert, D. L. 1995, PASP, 107, 251
Ulrich, R. K. 1972, ApJ, 172, 165
Wanajo, S., Nomoto, K., Iwamoto, N., Ishimaru, Y., & Beers, T. C. 2006, ApJ, 636, 842
Wanajo, S., Tamamura, M., Itoh, N., Nomoto, K., Ishimaru, Y., Beers, T. C., & Nozawa, S. 2003, ApJ, 593, 968
Wasserburg, G. J., Boothroyd, A. I., & Sackmann, I.-J. 1995, ApJ, 447, L37
Westin, J., Sneden, C., Gustafsson, B., & Cowan, J. J. 2000, ApJ, 530, 783
Wiese, W. L., Fuhr, J. R., & Deters, T. M., eds. 1996, Atomic Transition Probabilities of Carbon, Nitrogen, and Oxygen: A Critical Data Compilation (Washington, DC: American Chemical Society)
Yan, Z.-C., Tambasco, M., & Drake, G. W. F. 1998, Phys. Rev. A, 57, 1652
Zhang, H. W., & Zhao, G. 2005, MNRAS, 364, 712
Zijlstra, A. A. 2004, MNRAS, 348, L23
Zinner, E., Nittler, L. R., Gallino, R., Karakas, A. I., Lugaro, M., Straniero, O., & Lattanzio, J. C. 2006, ApJ, 650, 350